Government of Western Australia

Department of
Mines and Petroleum

REPORT 154

COBRA — AMADEUS BASIN PROJECT: GRAVITY AND MAGNETIC STUDY OF THE WESTERN AMADEUS BASIN, WESTERN AUSTRALIA

by C Foss, JR Austin, and S Schmid

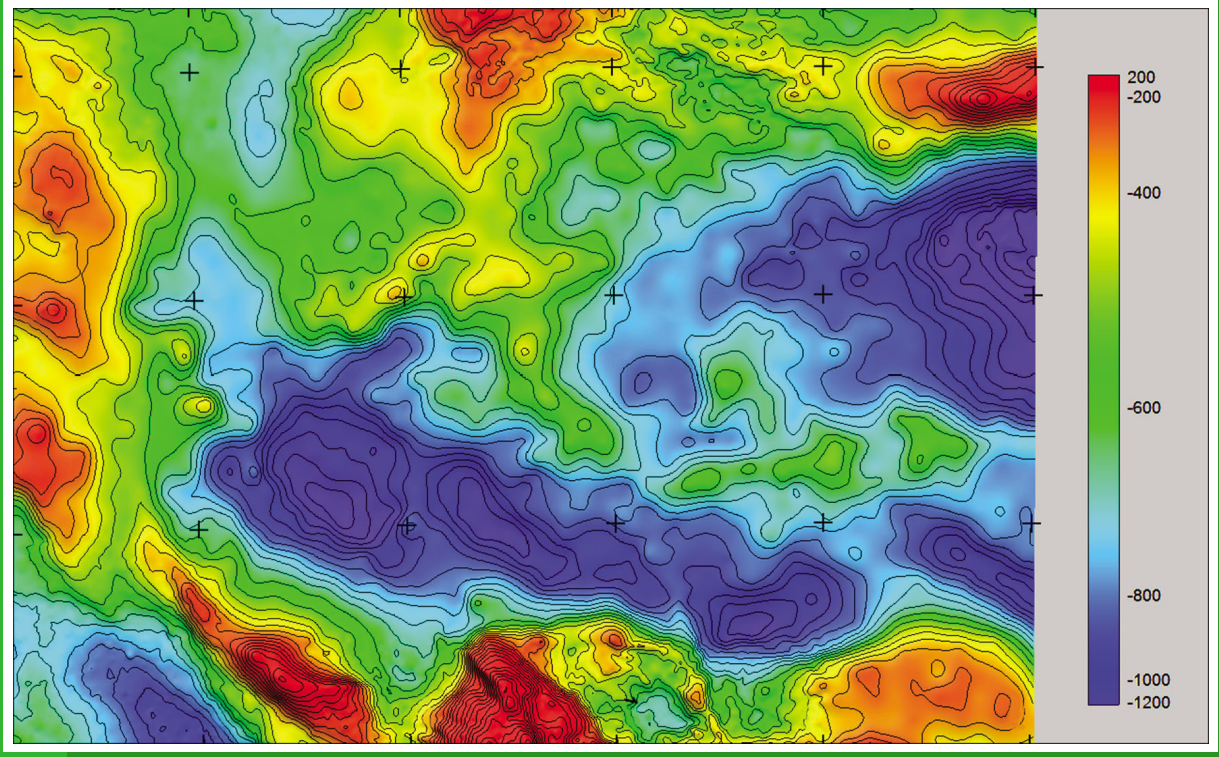

EXPLORATION INCENTIVE SCHEME

Geological Survey of Western Australia

Government of **Western Australia**
Department of **Mines and Petroleum**

REPORT 154

COBRA – AMADEUS BASIN PROJECT: GRAVITY AND MAGNETIC STUDY OF THE WESTERN AMADEUS BASIN, WESTERN AUSTRALIA

by
C Foss, JR Austin, and S Schmid

Perth 2015

Geological Survey of Western Australia

REFERENCE
The recommended reference for this publication is:
Foss, C, Austin, JR, and Schmid, S 2015 COBRA – Amadeus Basin Project: Gravity and Magnetic Study of the Western Amadeus Basin, Western Australia: Geological Survey of Western Australia, Report 154, 47p.

National Library of Australia Cataloguing-in-Publication entry:

Creator:	Foss, Clive, author.
Title:	COBRA - Amadeus Basin project, gravity and magnetic study of the western Amadeus Basin, Western Australia / Clive Foss, James Austin & Susanne Schmid.
ISBN:	9781741686425 (ebook)
Subjects:	Geophysics--Western Australia--Amadeus Basin. Geology--Western Australia--Amadeus Basin. Amadeus Basin (N.T. and W.A.)
Other Creators/Contributors:	Austin, J. R. (James R.), author. Schmid, Susanne, author. Geological Survey of Western Australia.
Dewey Decimal Classification:	559.4291

ISSN 1834–2280

Grid references in this publication refer to the Geocentric Datum of Australia 1994 (GDA94). Locations mentioned in the text are referenced using Map Grid Australia (MGA) coordinates, Zone 52. All locations are quoted to at least the nearest 100 m.

Published 2015 by Geological Survey of Western Australia
This Report is published in digital format (PDF) and is available online at <www.dmp.wa.gov.au/GSWApublications>.

Further details of geological publications and maps produced by the Geological Survey of Western Australia are available from:
Information Centre | Department of Mines and Petroleum | 100 Plain Street | EAST PERTH | WESTERN AUSTRALIA 6004
Telephone: +61 8 9222 3459 Facsimile: +61 8 9222 3444 **www.dmp.wa.gov.au/GSWApublications**

Cover photograph: Bouguer gravity grid (μm/s^2) over the western Amadeus Basin derived from Geophysical Archive Data Delivery System (GADDS) data

MINERAL RESOURCES FLAGSHIP
www.csiro.au

COBRA – Amadeus Basin Project

Gravity and Magnetic Study of the Western Amadeus Basin, Western Australia

Clive Foss, James Austin & Susanne Schmid

CSIRO EP: 15187

December 2014

Citation

Foss, Clive, Austin, James and Schmid, Susanne (2014). COBRA – Amadeus Basin Project, Gravity and Magnetic Study of the Western Amadeus Basin, West Australia.

EP 15187 CSIRO, Australia. p45.

Copyright and disclaimer

Important disclaimer

FOREWORD

This report describes a study of the western Amadeus Basin based primarily on interpretation of regional gravity and magnetic data. The primary objective of this study was to develop a feasible model of the basin container. The western section of the basin is not constrained by any deep seismic, basement-penetrating boreholes or magneto-telluric data, and interpretation at present is based substantially on the regional gravity and magnetic data, together with limited geological outcrop. The model which has been developed is therefore necessarily somewhat speculative. It has however been designed in a modular format, suitable for editing as and when any new constraints become available, or to test any alternative hypotheses of the basin structure.

Gravity and magnetic data, and their interpretation, are quite different to each other, and this has dictated the approach to this project, and controls what geological information can be recovered from the interpretation, and at what level of confidence. Measured magnetic field variations are entirely due to ferromagnetic minerals, which rarely exceed a few percent, even in rocks considered strongly magnetic. Many rocks do not generate detectable external magnetic fields, and cannot be directly mapped by magnetic field interpretation. The distribution of useful signal in the magnetic field is very irregular, but where it does occur, it can provide absolute estimates of depth to source of relatively high reliability and precision (generally to within +/- 15%). There is however still a geological interpretation to be made of what those sources are. Gravity field variation, on the other hand, is determined by the density of the underlying rocks; a physical property to which all parts of the rock contribute. Gravity field variations therefore typically arise from a wider range of geological sources. Steeply dipping density interfaces generate lateral gravity field variations, but it is difficult to recognise and resolve density contrasts across sub-horizontal interfaces. Interpretation of absolute depths from gravity interpretation is more difficult than for magnetics, and depends on assigned density contrast values, which in this study are unknown, or only poorly known. Gravity variation across the western Amadeus Basin may arise from density contrasts within the sedimentary section, from variations in basement depth, from lateral variations in basement density, and from any variation in crustal thickness beneath the basin. It is not possible to attribute measured gravity variations to these various sources without independent constraints, which are not presently available. The gravity modelling in this study is therefore highly interpretive.

The magnetic field data acquired on large regional surveys, on north-south lines at 400 metre spacing and terrain clearance of about 80 metres, maps the magnetic field adequately. The gravity data coverage across much of the study area is the original national 11 km spaced data, which provides limited constraint on the sharpness of the gravity field variations, and thereby limited discrimination of the depth of the relevant density contrasts. This inadequacy of the gravity data has been mitigated over the Rawlinson and MacDonald 1:250,000 map sheets by the availability of airborne gravity data, which has a resolution approximately equivalent to a ground station spacing of about 4 kilometres, and which clearly reveals greater geological signal in the gravity field than did the earlier 11 km spaced ground stations over the same area.

CONTENTS

FIGURES

ACKNOWLEDGMENTS

This Project was funded by CSIRO Mineral Resources Flagship (MRF), the Geological Surveys of Western Australia and the Northern Territory, and the company sponsors. We would like to thank our internal reviewers.

EXECUTIVE SUMMARY

This study of the Amadeus Basin proposes a structural model of the basin, consistent with present information. The objective of the study has been to develop this model as a starting point for, and input to, regional exploration for resources within the basin. There is no deep drilling within the western section of the basin, and very little deep seismic data. Most of our understanding of the basin structure depends on interpretation of regional gravity and magnetic data sets. This interpretation is by its nature intrinsically non-unique.

In this study, the magnetic field data provides clear mapping of the basin margin, as the limit of sharp, high-amplitude magnetic field variations due to outcropping or shallow sub-cropping strongly magnetised basement rocks. There are however relatively sparse magnetic field anomalies suitable for estimating depth from strongly magnetised rocks beneath the basin itself. Many of the depths which are determined are in excess of 10 kilometres, which is considered improbably deep for the base of the Amadeus section at the Heavitree/Dean Quartzite. This apparent discrepancy is explained by interpreting the magnetic source depths as marking an older and deeper crystalline basement surface, below a thick section of magnetically transparent sediments or metasediments which extend over large areas beneath the Amadeus Basin.

The basin model derived in this study is based primarily on interpretation of the gravity data. The deepest Amadeus Basin section modelled was in the far east of the study area, at depths in excess of 8 kilometres. That section thinned considerably towards the west, to less than 3 kilometres over a broad north-south basement ridge. The ridge is also marked by a north-south string of small, shallow magnetic sources, which are not believed to be within basement. In combination, the gravity model and derived magnetic source depths, appear to map an interface which extends to depths in excess of 10 kilometres, which across much of the basin is interpreted as the base of a pre-Amadeus section of sediments or meta-sediments.

The model has been generated in a modular format, so that it can be adjusted to accommodate any new constraints in the future, or to test alternative hypotheses.

1 INTRODUCTION

The Amadeus Basin is part of the Neoproterozoic Centralian Basin (Walters et al., 1995), which lies within the NT and WA, and covers over 170000 km^2. This project is part of the COBRA – Amadeus Basin Project that aims to assess the petroleum and mineral potential using a multi-disciplinary approach. The gravity/magnetics basin inversion that is subject of this report has the aim to help understanding the geology of the widely dune-covered part of the basin within Western Australia.

The geology of the Amadeus Basin comprises three packages divided by unconformities; 1) Neoproterozoic sedimentary and glacial rocks, 2) Cambrian to Carboniferous sedimentary rocks, and 3) Tertiary to recent sedimentary rocks. The current structural framework has been modified by salt tectonics, which may have been activated during the Petermann and/or Alice Springs Orogenies that have modified the basin. The thickness of the Amadeus Basin has previously been interpreted as containing an up to 14 km thick succession of sediments (Wells et al., 1970; Korsch and Lindsay, 1989). The basin mainly overlies metamorphic and igneous rocks of the Palaeo- to Mesoproterozoic Arunta and Musgrave Provinces. However, outcrops in the SW of the basin suggest that part of the basin is sitting on top of a late Mesoproterozoic sedimentary and volcanic rift basin (Korsch and Lindsay, 1989). Korsch and Lindsay (1989) interpreted the formation of the basin from an original rift phase with bimodal volcanism at 897 Ma. Thermal thinning of crust and sagging subsequently led to widespread sedimentation of the Heavitree/Dean Quartzite, now recognised as the oldest unit within the basin. The Petermann Orogeny (Ediacaran to Early Cambrian) and Alice Springs Orogeny (Late Devonian to Late Carboniferous, Haines et al., 2001) resulted in shortening of the basin and décollement between basement and basin. The shortening during the Petermann Orogeny is largely oriented NE-SW leading to NW-SE structures within the Neoproterozoic sedimentary succession, while the Alice Springs Orogeny structures are mostly E-W trending along the northern margin of the basin.

Little recent geophysical work happened in the western Amadeus Basin. However, there have been several studies on the surrounding basement areas. To the north, Joly et al. (2013) have applied gravity and magnetic interpretation, together with some detailed gravity traverse modelling to investigate crustal structure of the southwest Arunta Block, and speculate on its mineral prospectivity. To the south, there have been several studies of the crustal structure of parts of the Musgrave Block (for example, Aitken et al. 2013, Smithies et al. 2013, and Neumann 2013), using gravity and magnetic interpretation and modelling, magneto-telluric sounding, and a single deep seismic reflection line. Unfortunately, none of these studies extend across the Amadeus Basin margin, to provide substantial assistance with this study of basin structure.

Unravelling the basin architecture and advancing the understanding towards potential conventional hydrocarbon accumulations and sediment-hosted mineral systems was primary objective for this study.

2 GRAVITY AND MAGNETIC COVERAGE OF THE WESTERN AMADEUS BASIN

The gravity data used in this study is a combination of land gravity stations downloaded from the Geoscience Australia Geophysical Archive Data Delivery System (GADDS), and airborne gravity data from a survey flown for Central Petroleum in 2008. The distribution of the land gravity stations and airborne gravity survey flight lines is shown in Figure 1. The westernmost part of the basin is only covered with stations at a nominal 11 km spacing, and this sparse coverage limits the information which can be recovered from the gravity field. The section of the basin immediately to the east of the West Australia/ Northern Territory (along 129˚ east) border has substantially improved coverage from an airborne gravity survey, and far greater geological structure is evident in the gravity images over this survey area. Much of the Arunta Block to the north has stations at 2.5 km spacing.

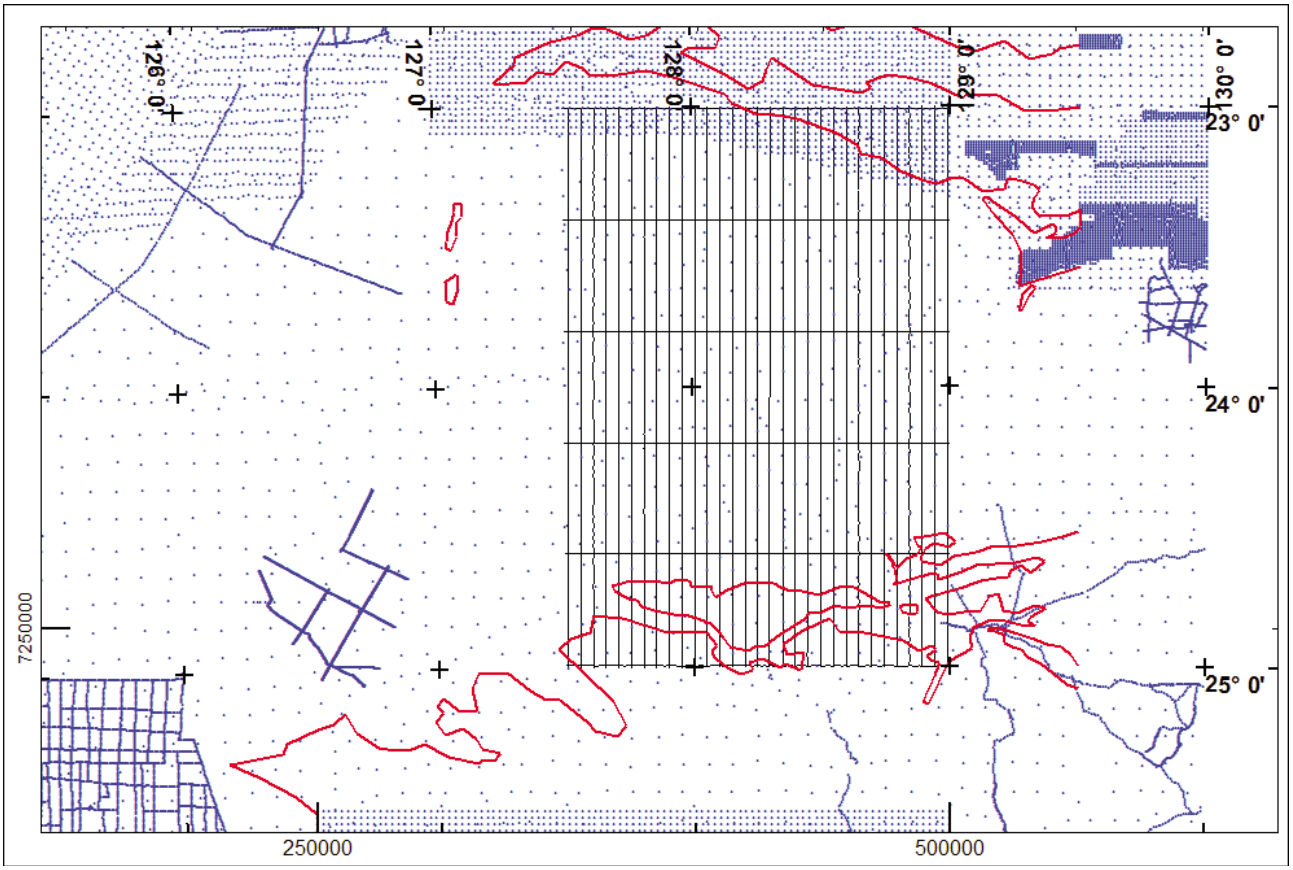

Figure 1. Distribution of gravity stations (blue) and airborne gravity lines (black), with basin margins interpreted from magnetics (red). All maps are shown in the GDA zone 52 projection and latitude/longitude.

2.1 Geophysical Archive Data Delivery System (GADDS) gravity data

The Bouguer gravity variation is imaged in Figure 2. The range in gravity across this section of the basin is approximately 700 µm/s^2 (70 mGal). Factors contributing to this gravity variation are likely to be:

1) Variation in basement depth, with a density contrast between the basin fill and the underlying basement
2) Lateral variation in density of the basement rocks
3) Variation in density of the infilling sediments (particularly between salt-dominated formations and clastic or carbonate dominated formations

4) Variation in crustal thickness beneath the basin.

The GADDS gravity data are a compilation of many different surveys. Geoscience Australia provides quality control on this data, but verification is very difficult, particularly because the gravity meters used measure relative variations in gravity, and between many of the surveys there are no common stations at which to establish a consistent datum. The 11 kilometre spaced data, which covers much of the western section of the basin, is from a national survey using helicopter support. Station locations were determined from aerial photographs, without accurate surveying, and station elevations were determined by barometric altimetry, with substantial resulting errors in the processed gravity values.

The various possible contributions of gravity variation are discussed in section 5 on gravity modelling. There are discrete and high amplitude gravity highs over outcropping and sub-cropping high-density units within the Arunta and Musgrave Blocks to the north and south of the basin, and the edges of these units are marked by much more substantial gravity gradients than are the edges of the basin. The main gravity low, which marks the basin in the Northern Territory, has substantially reduced amplitude compared to the eastern section of the basin, and there is a thin, disrupted gravity high which may mark the junction between the Amadeus and the younger Canning Basin to the West. There is a substantial gravity low to the north-west margin of the Musgrave Block, and similar, but smaller and dislocated gravity lows to the east, over the Musgrave Block. Linear trends are evident across the gravity image, with NW-SE and NNE-SSW trends dominant.

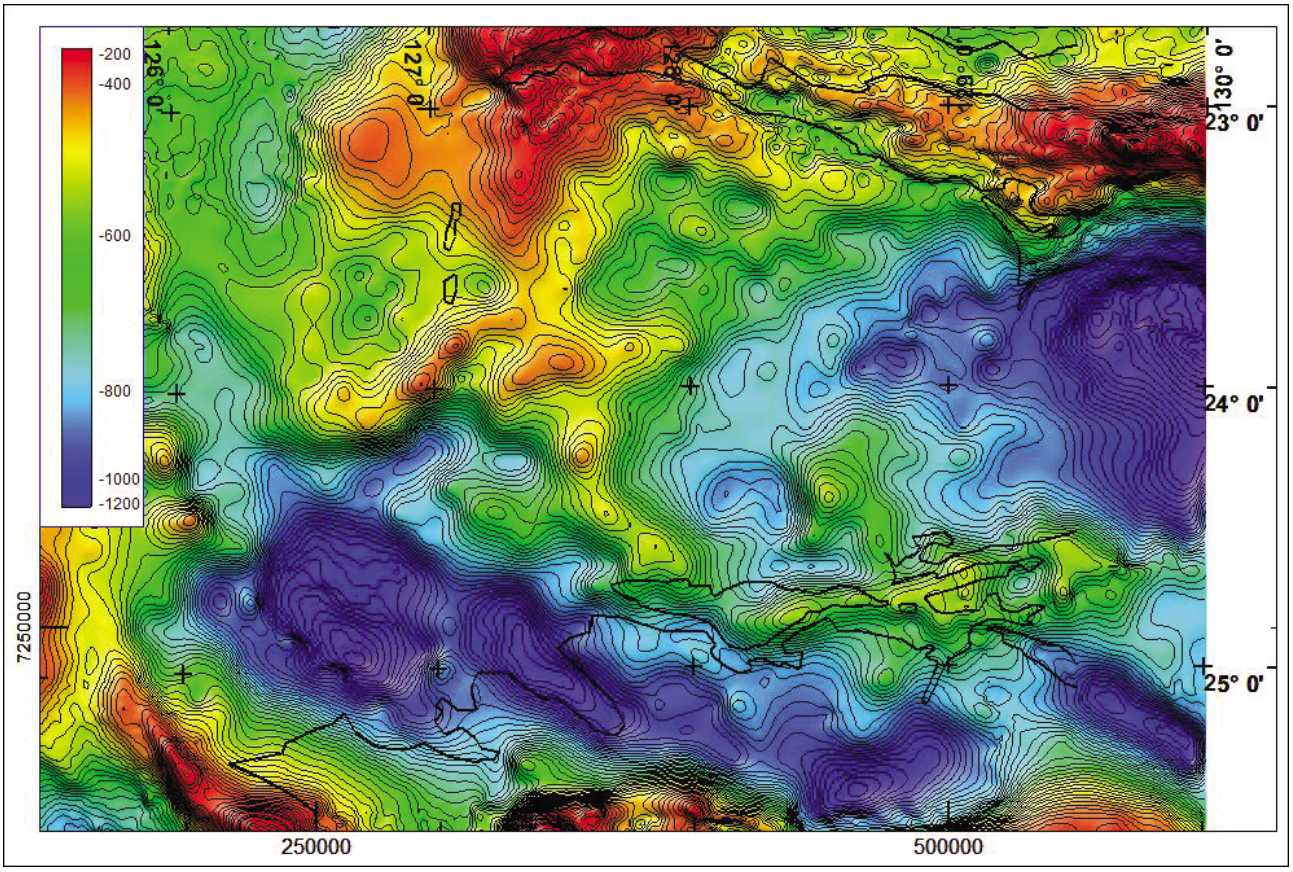

Figure 2. Bouguer gravity (µm/s²) grid derived from GADDS data. The vector overlay (in black) shows the magnetic field interpretation of the basin margin.

Figure 3 shows the vertical derivative enhancement of the gravity field. This filter amplifies the expression of the shallowest density variations, here mostly interpreted as due to the density contrast across the top of basement. The gravity expression of the edge of the basin is more prominent in this image than in the Bouguer gravity image, as are many of the NW-SE and NE-SW trends, suggesting that those may in part be the expression of faulting across which there is some vertical displacement of the basement surface. Unfortunately, however, the image is disrupted by grid

curvature artefacts over those areas with sparse gravity measurements. Some of the discrete gravity lows over the basin might mark salt features, but this cannot be established because many are due to individual gravity stations.

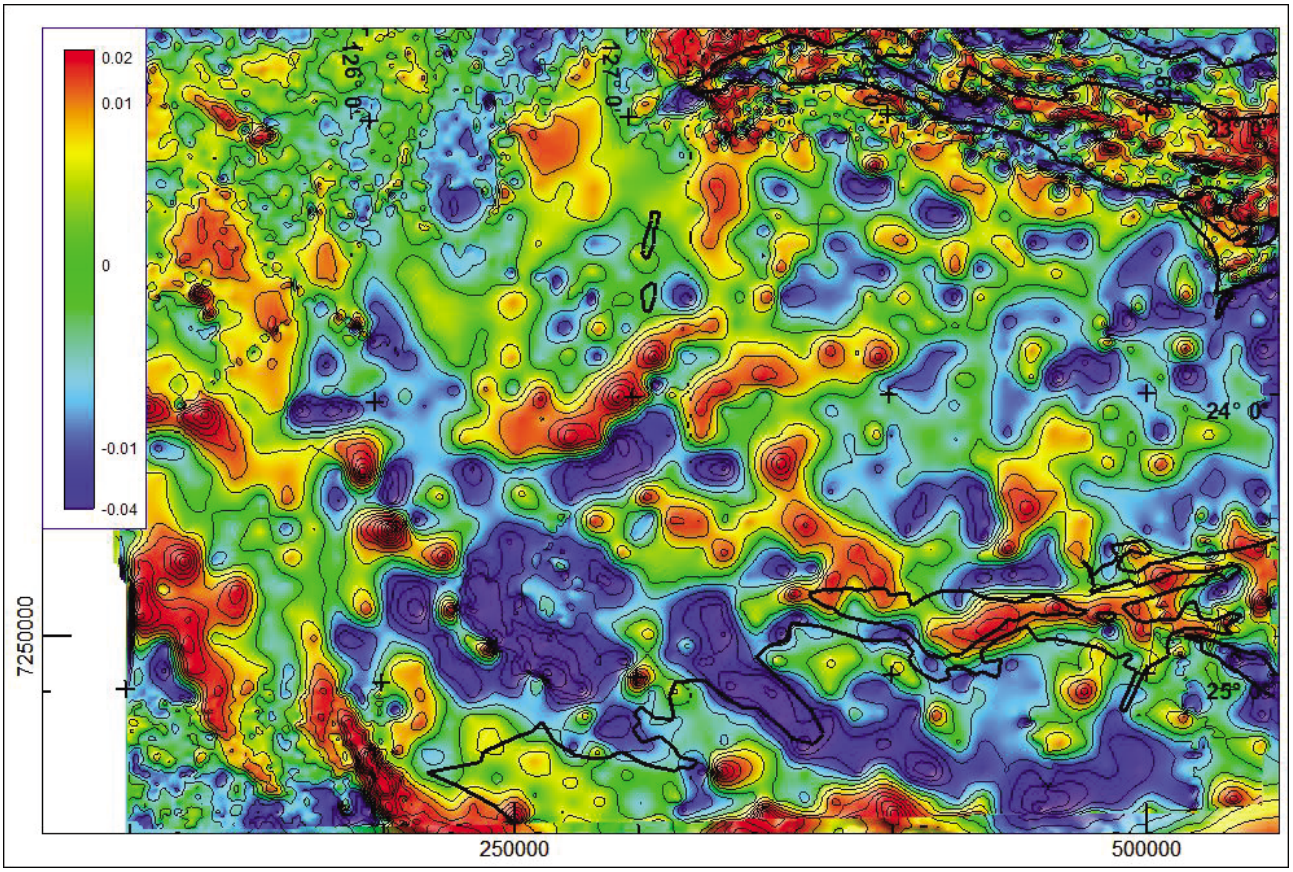

Figure 3. First vertical derivative of GADDS Bouguer gravity (preconditioned with an upward continuation to reduce the curvature effects at the sparse data points). Units are Eotvos x10^{-3}.

2.2 Central Petroleum 2012 Airborne Gravity Survey data

From May to July 2008 Airborne Petroleum Geophysics flew an airborne gravity survey of almost 8000 line kilometres for Central Petroleum. The survey covered the 1:250,000 Rawlinson and MacDonald map sheets. The flight line map is shown in Figure 1. The survey was flown using a GT-1A gravity meter (serial number S/N007) on north-south flight lines at 5 km spacing, with east- west tie lines at 44 km line spacing. The survey was flown at an elevation of 1200 m above sea level. Figure 4 shows Bouguer gravity over the survey area derived from the GADDS ground gravity stations (on the left), and derived from the airborne gravity survey data (on the right). There is good general agreement between the two images, but clearly the airborne survey provides a substantially higher resolution coverage. This difference in resolution of the two datasets is further highlighted in Figure 5, which compares the vertical derivative enhancements of Bouguer gravity.

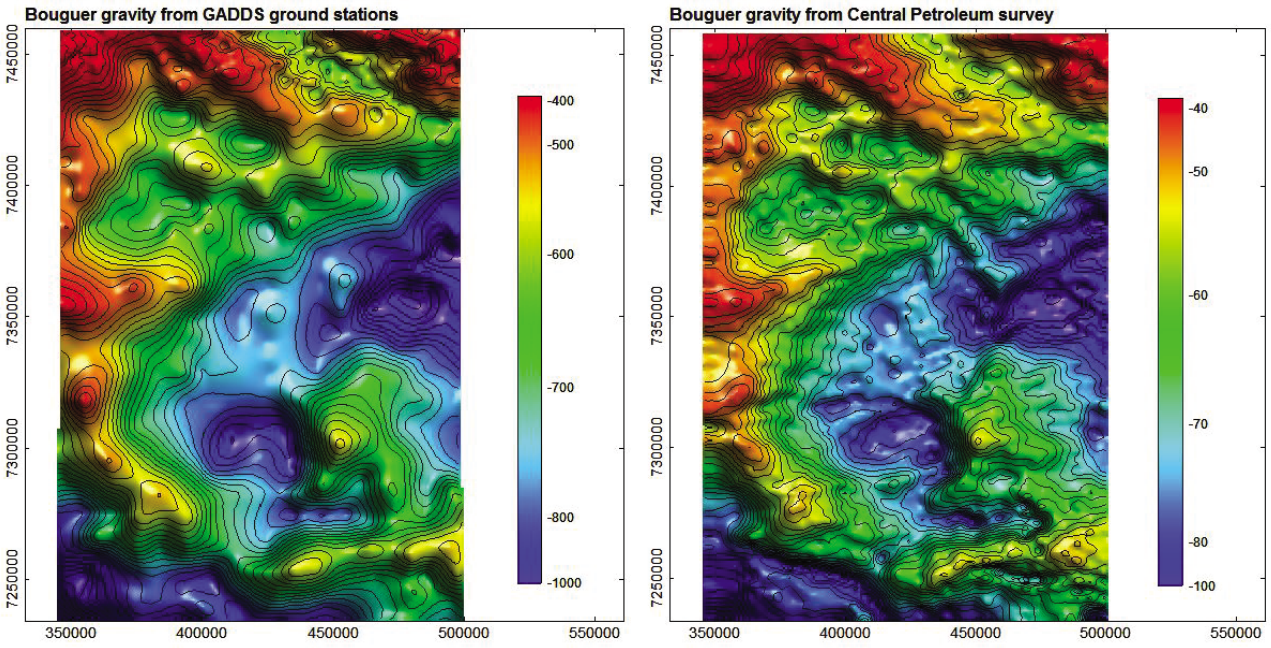

Figure 4. Comparison of Bouguer gravity from the GADDS ground stations (left) and the Central Petroleum airborne survey (right). Units are μm/s².

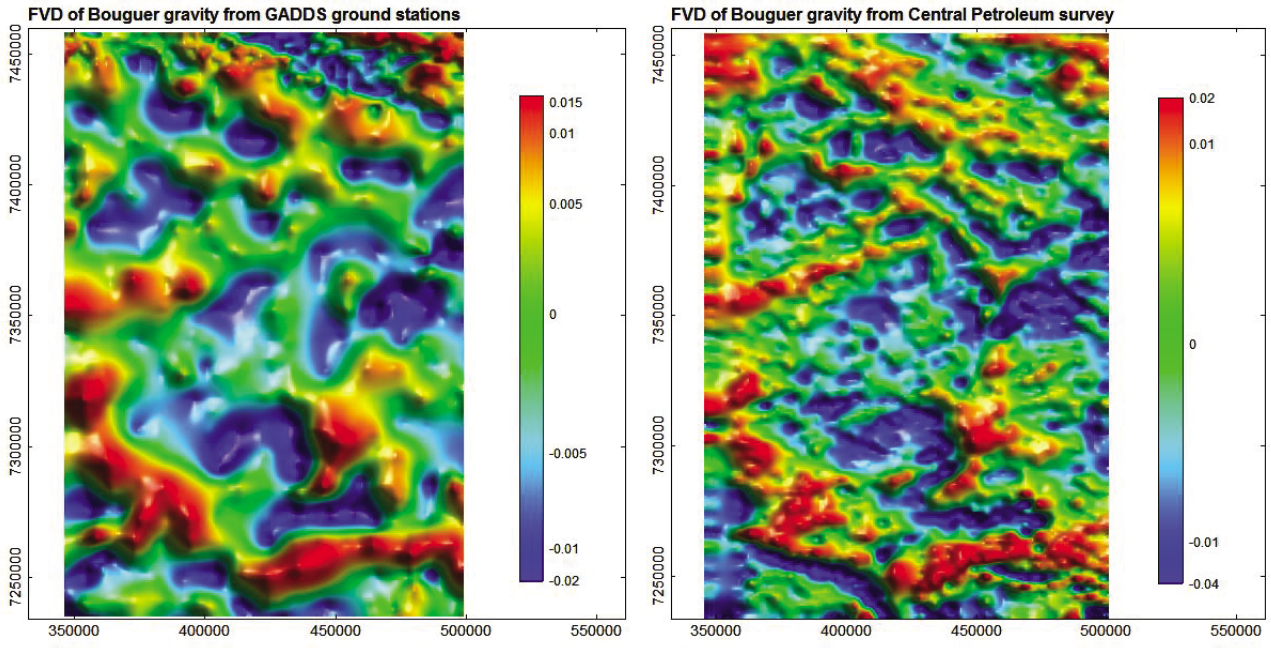

Figure 5. Comparison of the vertical derivative of Bouguer gravity from the GADDS ground stations (left) and the Central Petroleum airborne survey (right). Units are Eotvos x 10⁻³.

A merge of the vertical derivative enhancement of Bouguer gravity from the GADDS data, with replacement by the higher resolution vertical derivative enhancement of the airborne Bouguer gravity data over the airborne survey area is shown in Figure 6. Trends seen in the airborne survey data can be seen to extend over the surrounding regions, but at lower resolution. Care must be taken in interpretation of this image, because the mapped variation is a compound of geological signals, and lateral variation in data density. Nevertheless, the airborne gravity data in particular, emphatically shows shallow structure, due either to basement topography, and/or density variations within the basin section (which most probably include salt features). Many of the thinner linear features are relative gravity highs, most easily interpreted as horst blocks (because thin linear features over salt tectonics would be expected to be predominantly negative amplitude features over low-density salt walls).

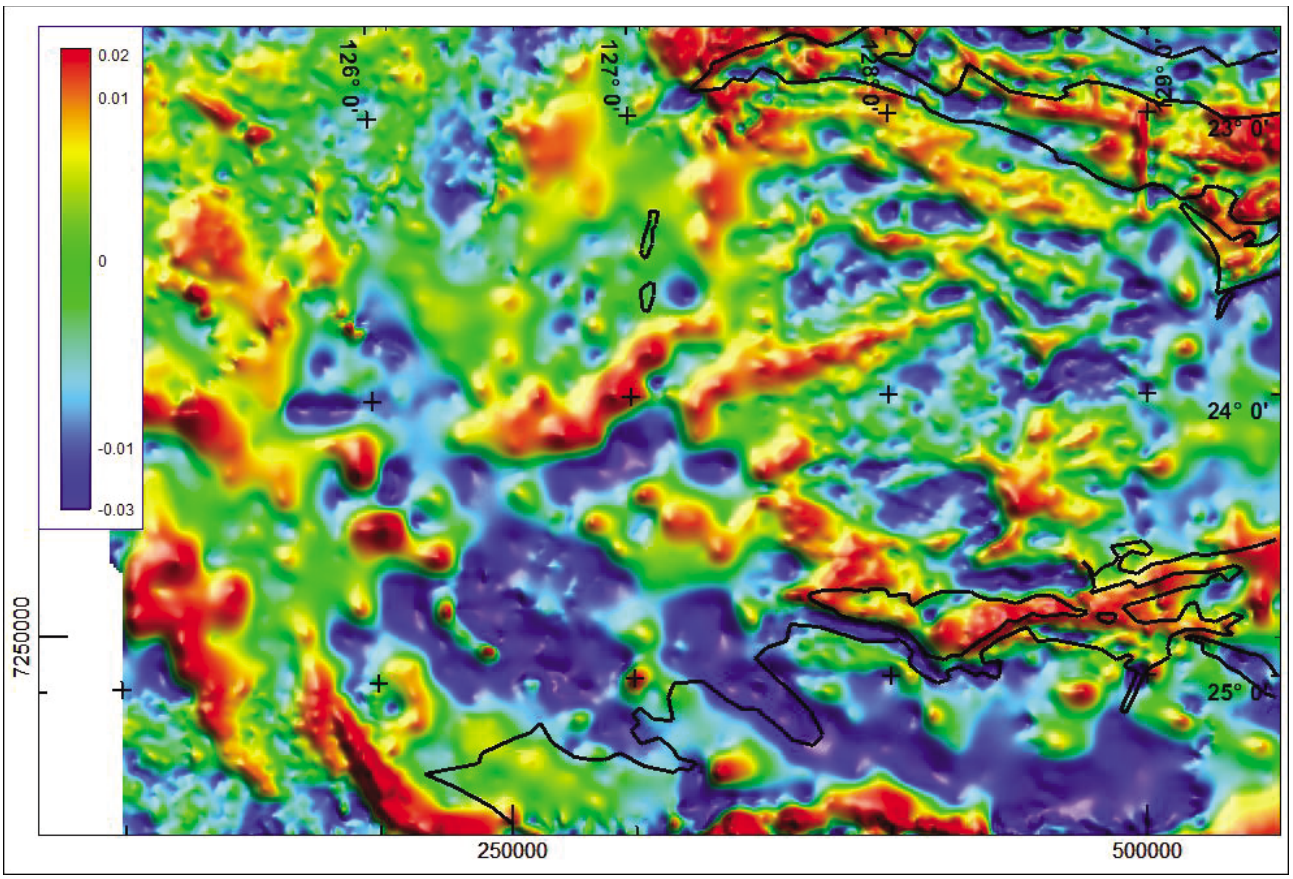

Figure 6. Combined GADDS and Central Petroleum Bouguer gravity first vertical derivative (with 500 m upward continuation pre-conditioning). Units are Eotvos x 10^{-3}.

A regional merge of these two data enhancements is shown in Figure 7 (note that a higher resolution mapping of the area immediately to the east of the airborne gravity survey will shortly become available, with infill of the existing gravity coverage of that area from 11 km spaced stations, down to spacing of 4 km and two kilometres in some areas).

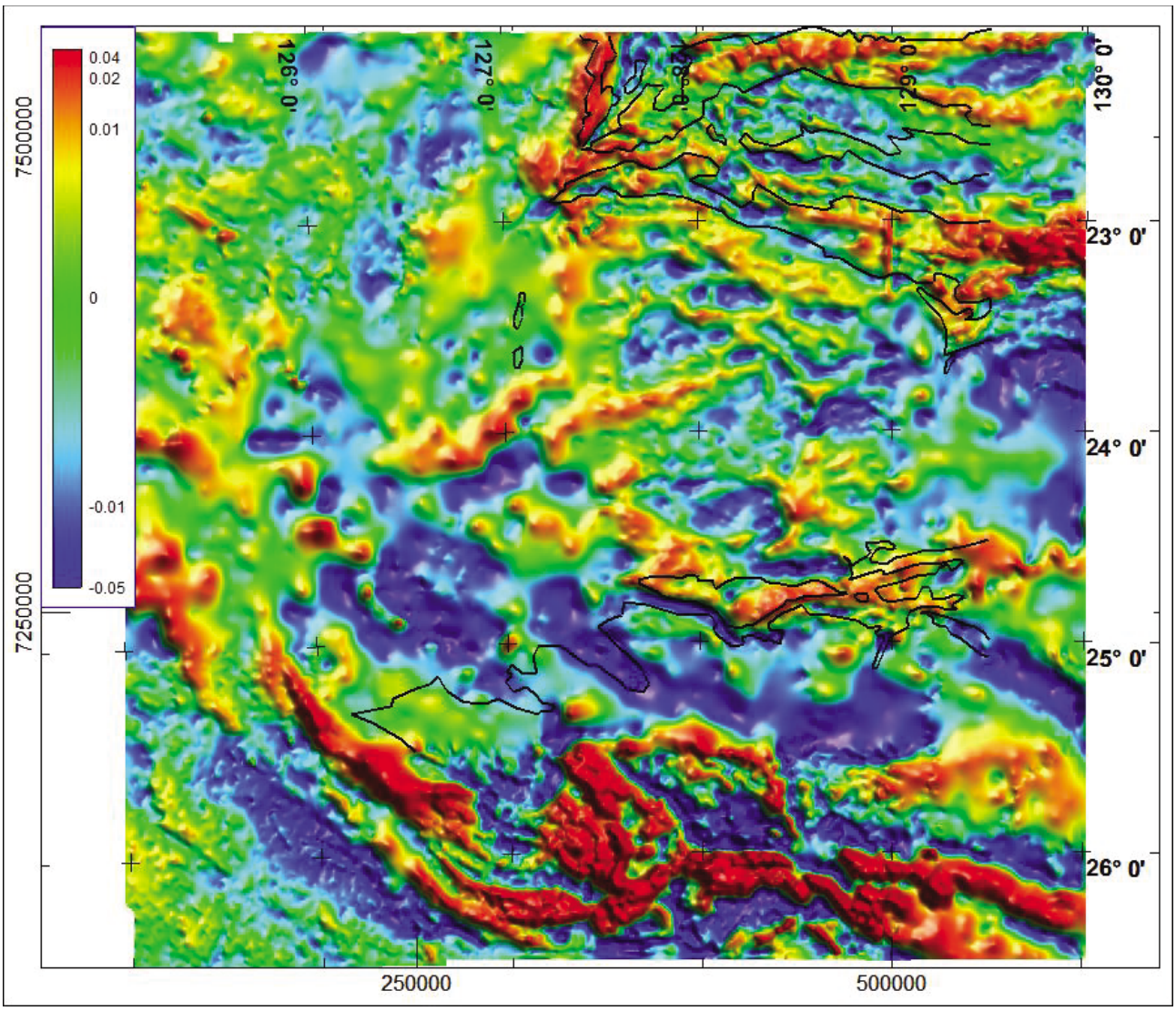

Figure 7. Combined vertical derivative of GADDS and Central Petroleum Bouguer gravity. Units are Eotvos x 10^{-3}.

2.3 Geophysical Archive Data Delivery System (GADDS) aeromagnetic data

The magnetic field coverage over the western Amadeus Basin is far more uniform and sufficient than the corresponding gravity coverage. The basin is completely covered by surveys with north-south flight lines, at 400 metre line spacing, and a nominal terrain clearance of between 60 and 100 metres. Three surveys cover this western section of the basin: the 1993 MacDonald - Jolly Peaks survey (400 m line spacing, 60 m terrain clearance), the 1998 Rawlinson survey (400 m line spacing, 80 m terrain clearance), and the 2010 South Canning 2 Morris Cobb survey (400 m line spacing, 60 m terrain clearance). Line data for these surveys were downloaded from GADDS and gridded to a cell size of 80 m (1/5th of the line spacing).

An image of the magnetic field, including the region around the basin, is shown in Figure 8. This image was generated from the 2010 5th edition 80 m cell size national TMI grid, downloaded from GADDS. The image shows sharp, high amplitude magnetic field variations over both the Musgrave and Arunta blocks, with the Amadeus Basin characterised by very broad, smooth anomalies, and low-amplitude, sharp, curvilinear anomalies. The broad anomalies are generated by strong basement magnetisations at depth, and the sharp, curvilinear anomalies are generated by near-surface intra-sedimentary magnetisations. The strongest magnetic anomalies are over the southern Arunta Block, and these appear to continue to depth beneath the basin, from sources downthrown sequentially to the south. The rocks of the Musgrave

Block to the south are generally of weaker magnetisation, and over the southern part of the Amadeus basin there are fewer magnetic anomalies from buried basement sources from which to generate magnetic depth estimates. A discontinuous, north-south string of magnetic anomalies marks the interpreted transition between the Amadeus and southeast Canning basins. The background magnetic field values are higher to the east of this line than to the west of it, suggesting that the Amadeus Basin is underlain by a different, more magnetic basement than that beneath the eastern Canning Basin.

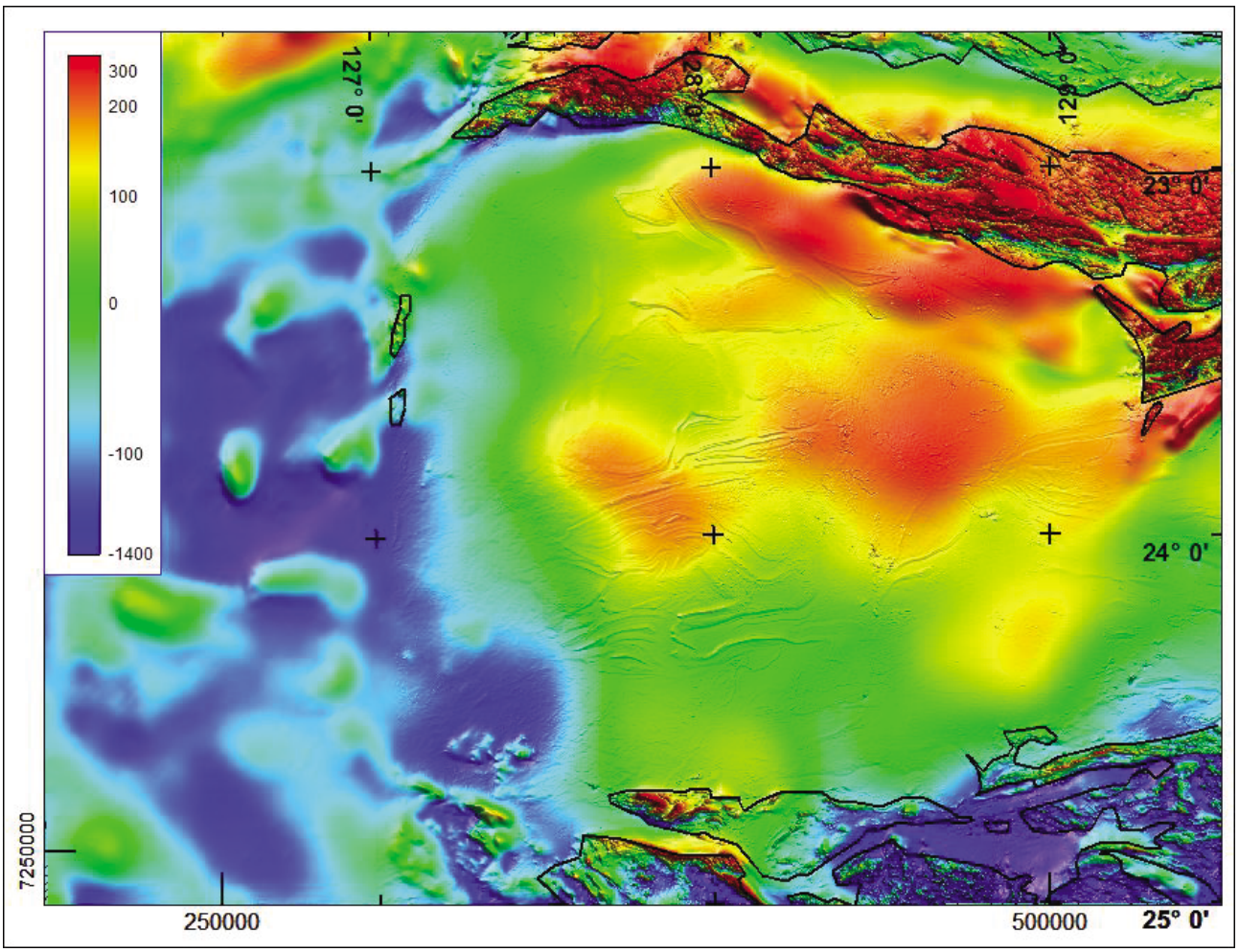

Figure 8. Total Magnetic Intensity (TMI) from GADDS 2010 national compilation grid with overlay of basin margin interpreted from the magnetic data. Units are nT.

A greyscale image of the vertical derivative of TMI is shown in Figure 9. This enhancement strongly accentuates the magnetic field contributions from shallow sources, and in particular the intra-sedimentary sourced anomalies. The apparent textural transition at the western edge of the Amadeus Basin is an artefact due to the fact that the 5th edition of the national grid from which this image was generated, did not include the most recent high-resolution survey over the western part of the project area. 127° east is an unfortunate transition between surveys, as it broadly coincides with a north-south trending set of magnetic features which appear to mark the transition between the Amadeus and eastern Canning basins. These anomalies can be explained as due to bodies entrapped in a fault zone, but this interpretation is highly speculative.

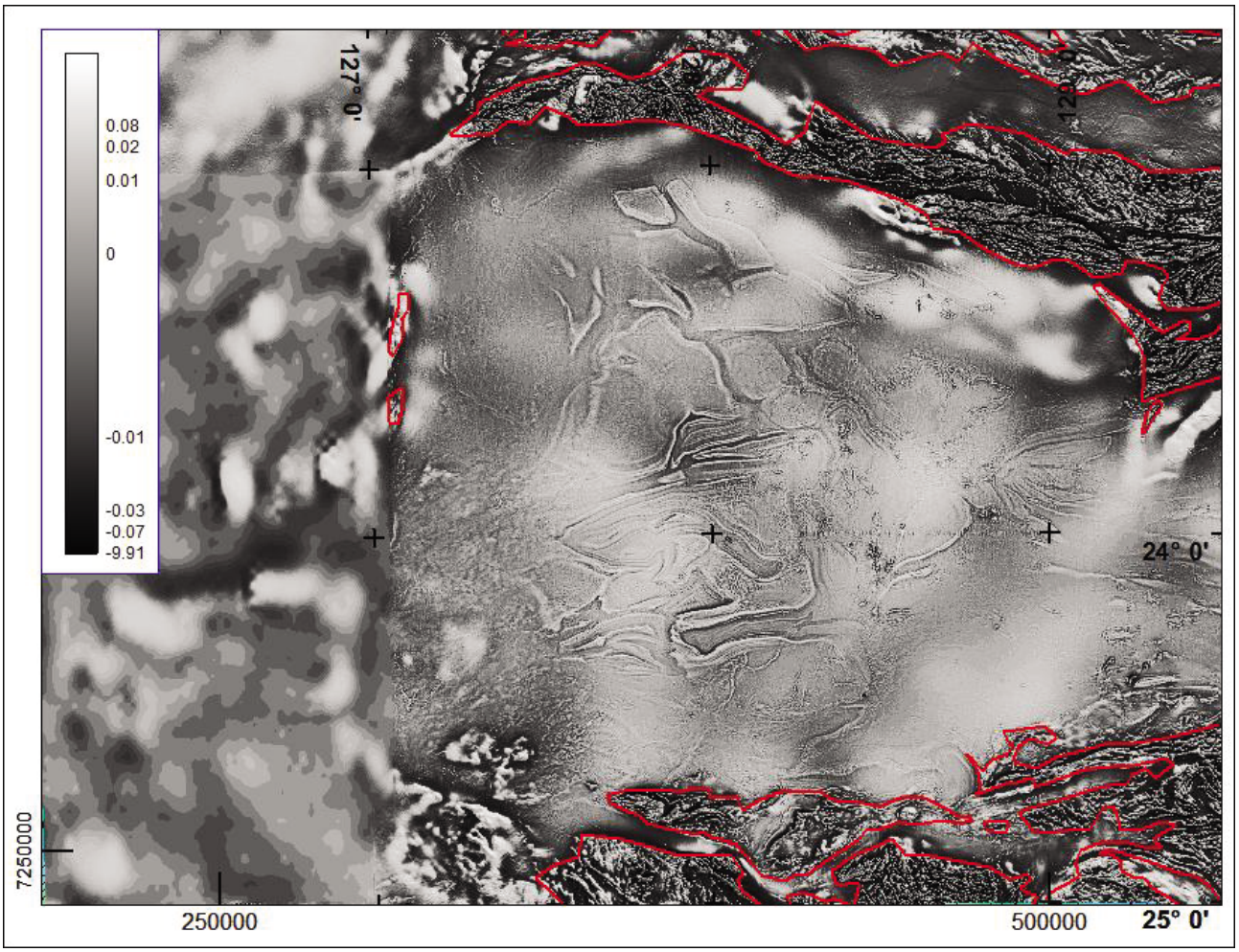

Figure 9. Greyscale first vertical derivative of TMI with overlay of basin margin interpreted from the magnetic data. Units are nT/m.

3 MAGNETIC FIELD MAPPING OF THE BASIN MARGINS

Sparse outcrop restricts geological mapping of the margin of the Amadeus Basin. Possibly the most continuous and reliable mapping of the margins of the basin are from the magnetic field data. In particular, the magnetic field data readily traces continuity of shallow magnetic sources, where moderately to strongly magnetised basement dips gradually beneath shallow cover. Also, where such shallow magnetisations are sharply truncated by any basement bounding faults, they give rise to characteristic magnetic anomalies. The major challenge in mapping basement from the magnetic field data, is that the basement is inhomogeneous, and in places consists of units such as felsic gneisses, granitoids and quartzites, which may have weak or negligible magnetic field expression, and can therefore be misinterpreted as part of the basin. Figure 10 shows the location of subsequent figures selected to highlight the mapping of the basin margin from the magnetic field data, superimposed on a terrain image generated from Shuttle Radar Topography Mission (SRTM) data. While the margin of the basin does in places coincide with topographic features, there is no clear relationship by which the margin could be derived from the terrain data.

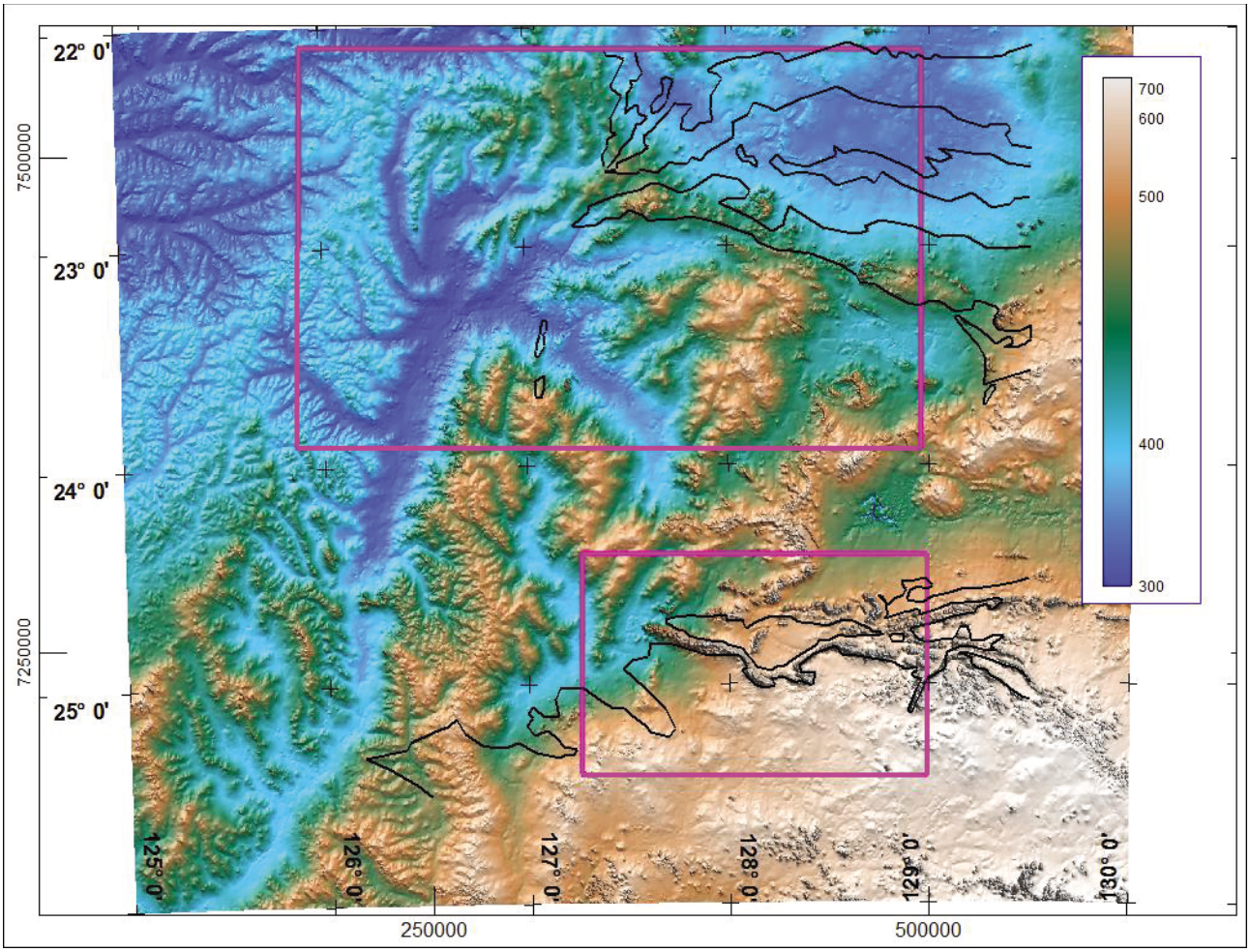

Figure 10. Southern and Northern Margin Focus Areas over digital terrain model. Units are metres.

3.1 Magnetic field mapping of the southern basin margin

A vertical derivative of TMI image over a section of the western margin of the basin is shown in Figure 11. This is the data from which the basin margin has been mapped. In places the termination of the high-amplitude, short-wavelength anomalies is abrupt, and the mapping of the margin is clear cut. However, the margin appears embayed, and with some isolated anomalies, suggesting that the basement surface dips only shallowly and irregularly to the north.

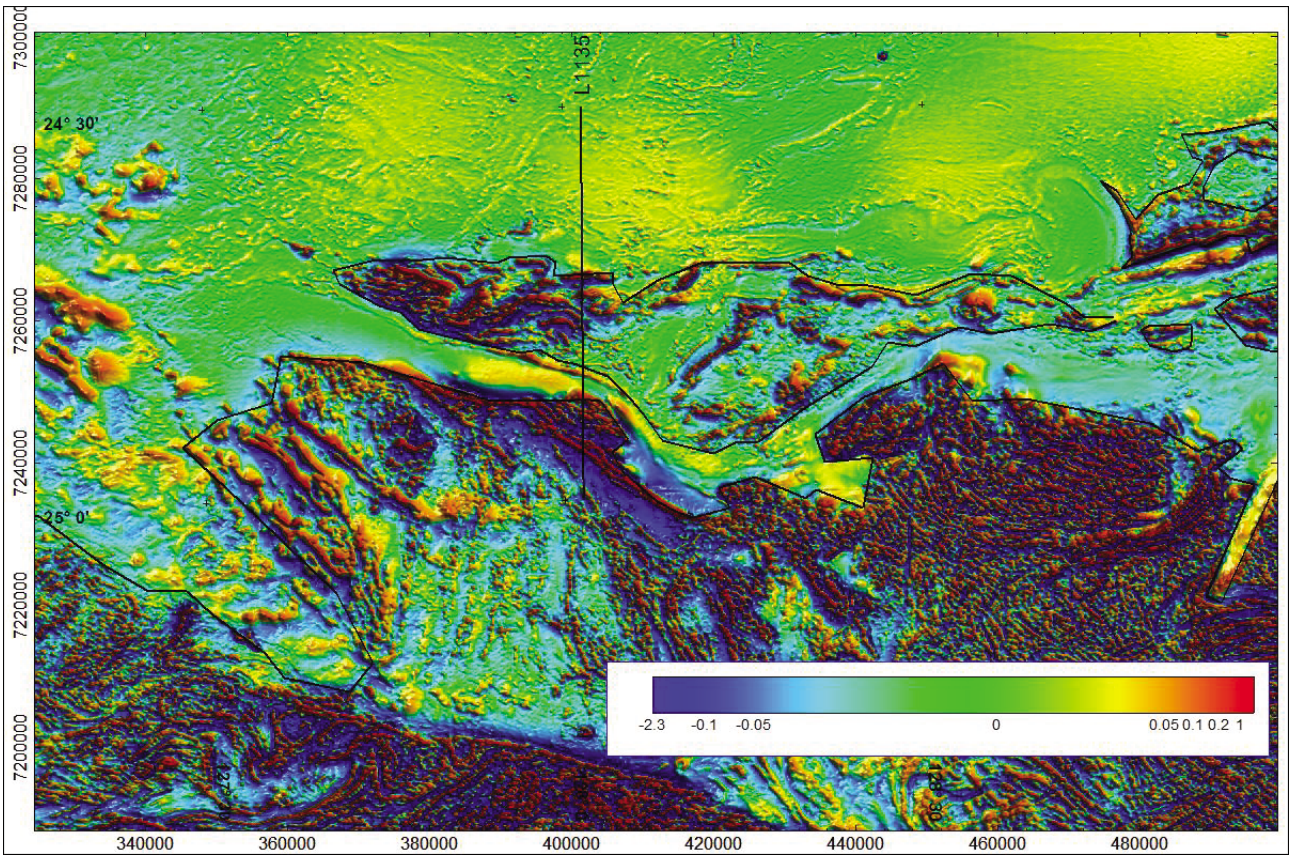

Figure 11. Southern margin vertical derivative of TMI. Units are nT/m.

The corresponding vertical derivative of gravity image is shown in Figure 12. The northern half of this area is covered by the Central Petroleum airborne gravity survey, which provides data of moderate to high resolution, suitable for the first vertical derivative enhancement. There is a sharp, linear gravity low over the Dean Quartzite in the Rawlinson Range. The steep gravity gradients suggest that this might be a rift, or possibly a half-graben. A similar, though less prominent, gravity low to the east may either be a fault-displaced extension of this feature, or an isolated rift. There is also a similar, east-west trending sharp, asymmetric gravity low immediately to the north of the basin margin as mapped from the magnetics, which also may possibly be due to a half-graben (with the steepest down-throw fault to the north). A much broader northwest-southeast trending set of linear gravity lows to the south correspond to an interpreted embayment as mapped from magnetics, may also be due to thick sections of low density sedimentary or meta-sedimentary rocks, but unfortunately this region is only covered by gravity data at an 11 km station spacing, which does not reveal details in the gravity field which would better support an interpretation.

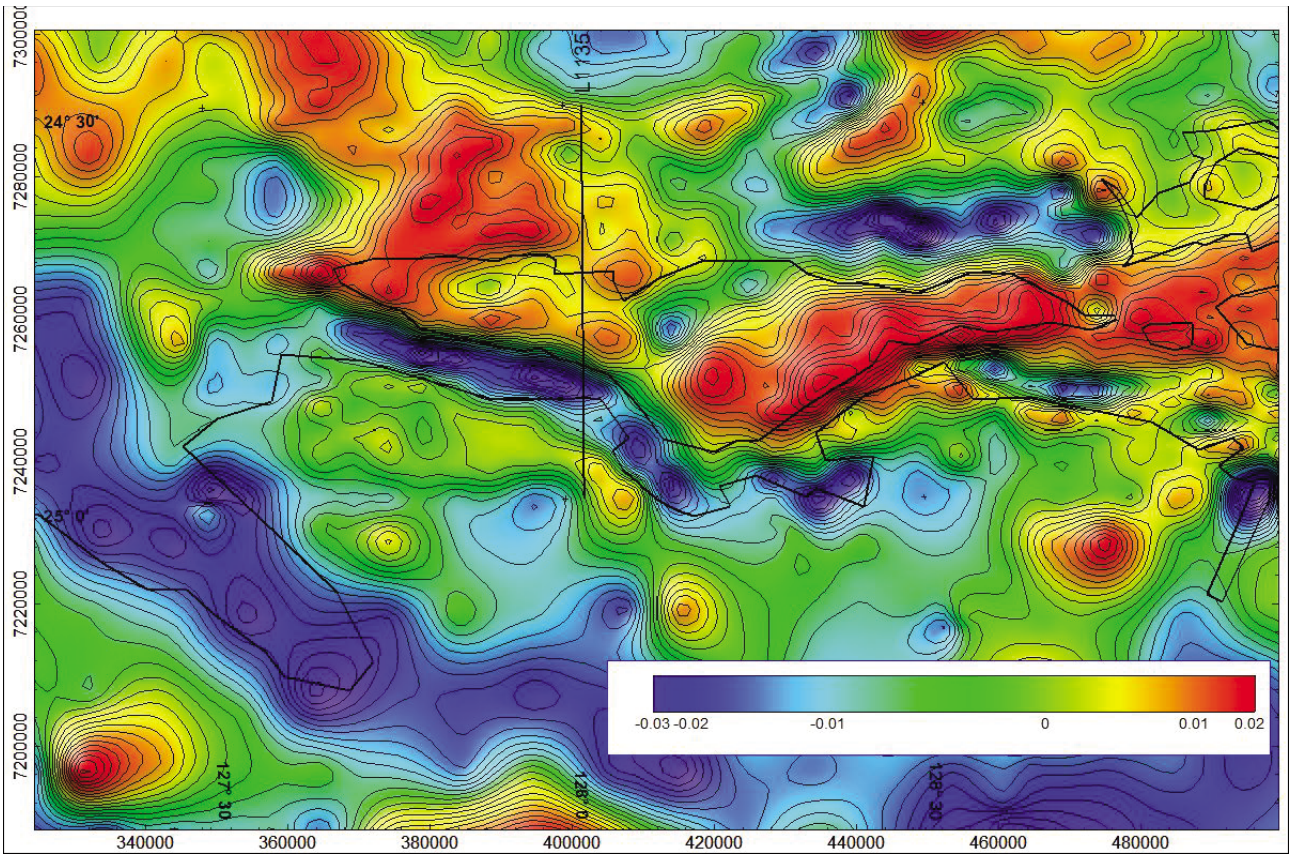

Figure 12. Southern margin vertical derivative of Bouguer Gravity (with 500 metre upward continuation).Units are Eotvos x 10^{-3}.

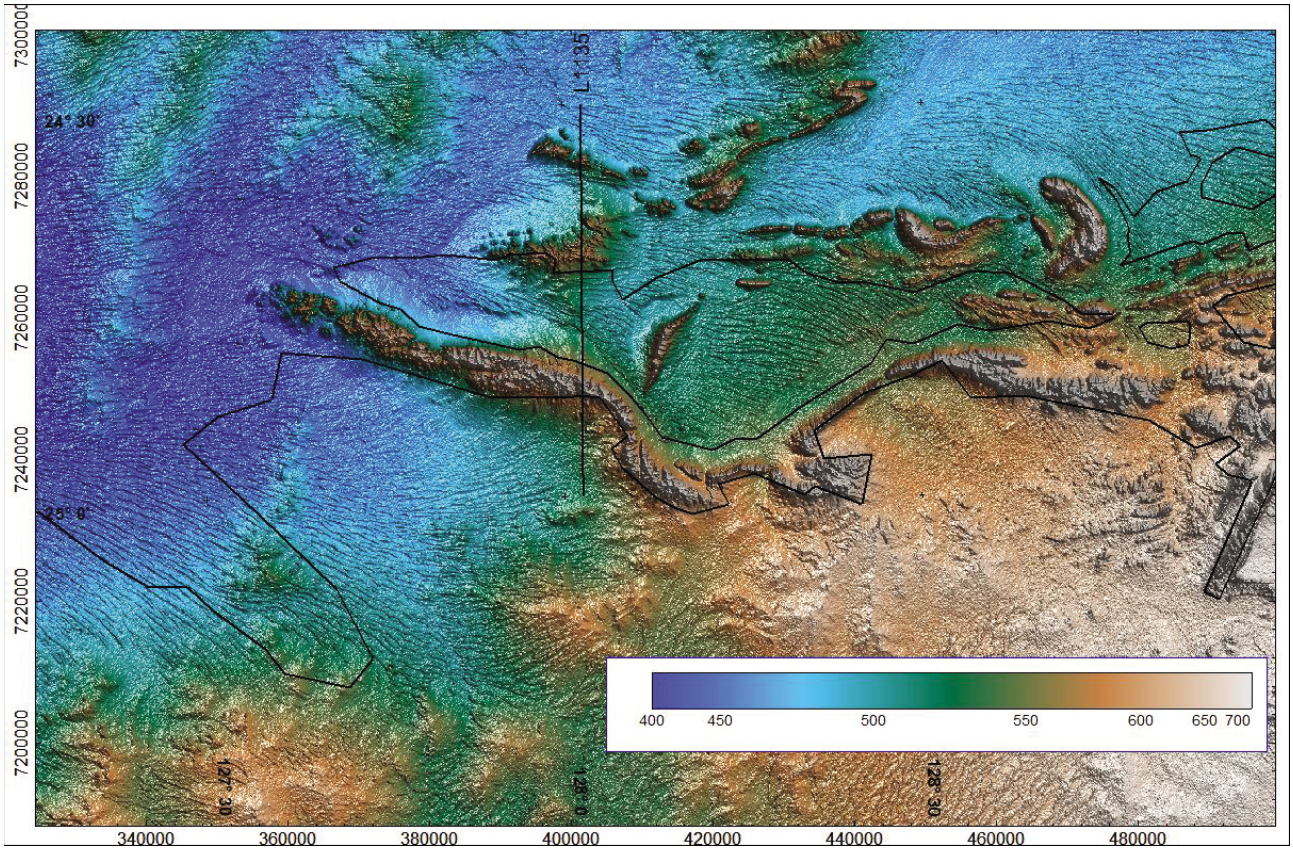

Figure 13. Southern margin digital terrain model.Units are metres.

The digital terrain image derived from SRTM data, shown in Figure 13, reveals a topographic inversion over the Dean Quartzite in the Rawlinson Range, and over those same sediments and the Dixon Range Beds north of the southern basin margin as mapped from magnetics. As shown in the Rawlinson 1:250,000 scale geological map in Figure 14, these areas of steep terrain provide almost the only control on bedrock geology. The localised, abrupt, steep gradients in the gravity data suggest that over the Musgrave Block, and immediately to the north of it, vertical block faulting is more significant than broad scale folding as shown in the 1:250,000 scale geological map sheet section.

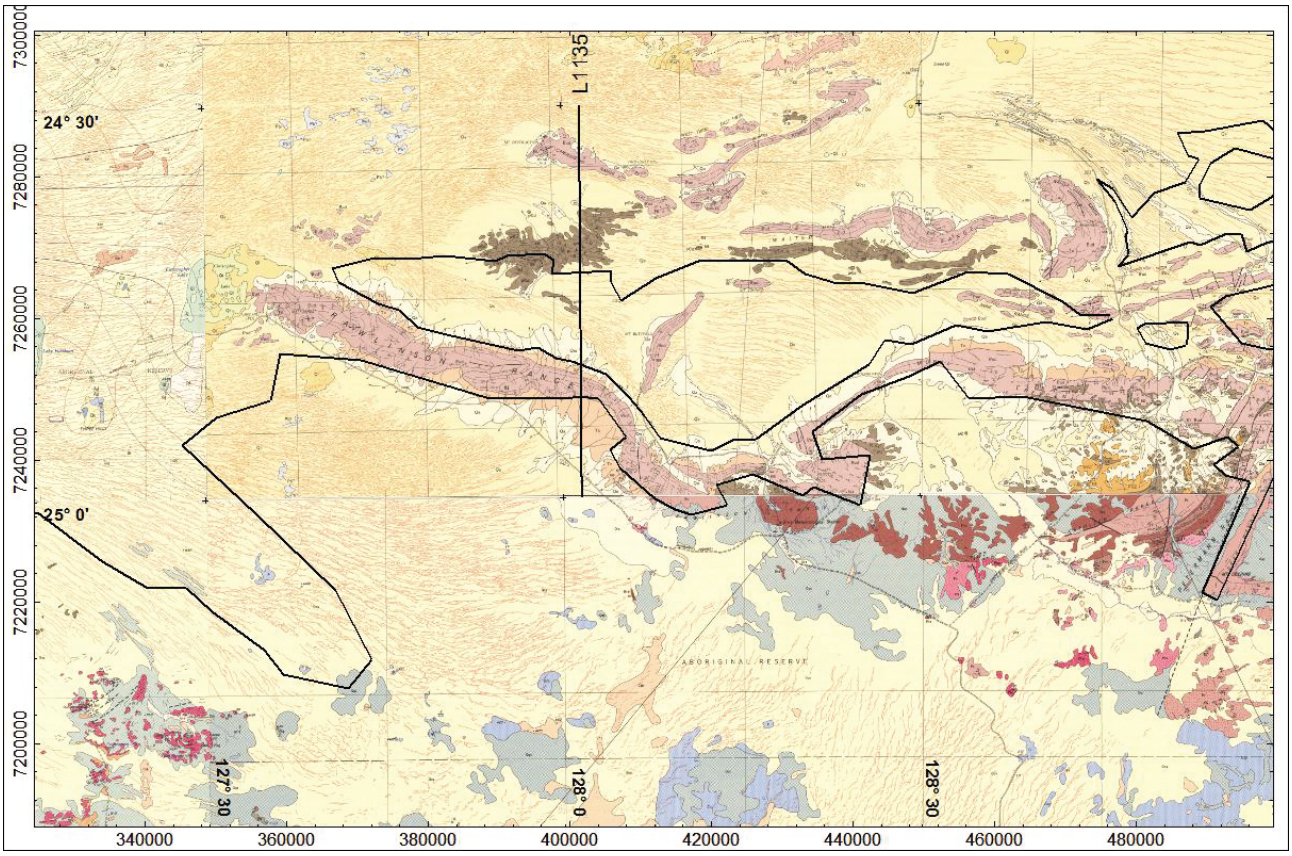

Figure 14. Southern margin overlay of basin margin interpreted from magnetic data over geological map.

A north-south flight line over the southern basin margin has been modelled as shown in Figure 15. There is a range of over 1000 nT, mostly due to sharp field variations over the southern third of the line. These variations can be well explained as due to thin units, mostly steeply dipping to north, and with magnetic susceptibilities of up to 0.4 SI. The top of the magnetic bodies are believed to trace the basement unconformity surface, beneath a magnetically transparent cover. Low amplitude variations over the Dean Quartzite of the Rawlinson Range appear to be sourced at depths of 1 km or less, and are most likely due to small-volume magnetisations within the sedimentary section, because the pronounced negative gravity anomaly over this area suggests that the thickness of the sediments is in excess of several kilometres.

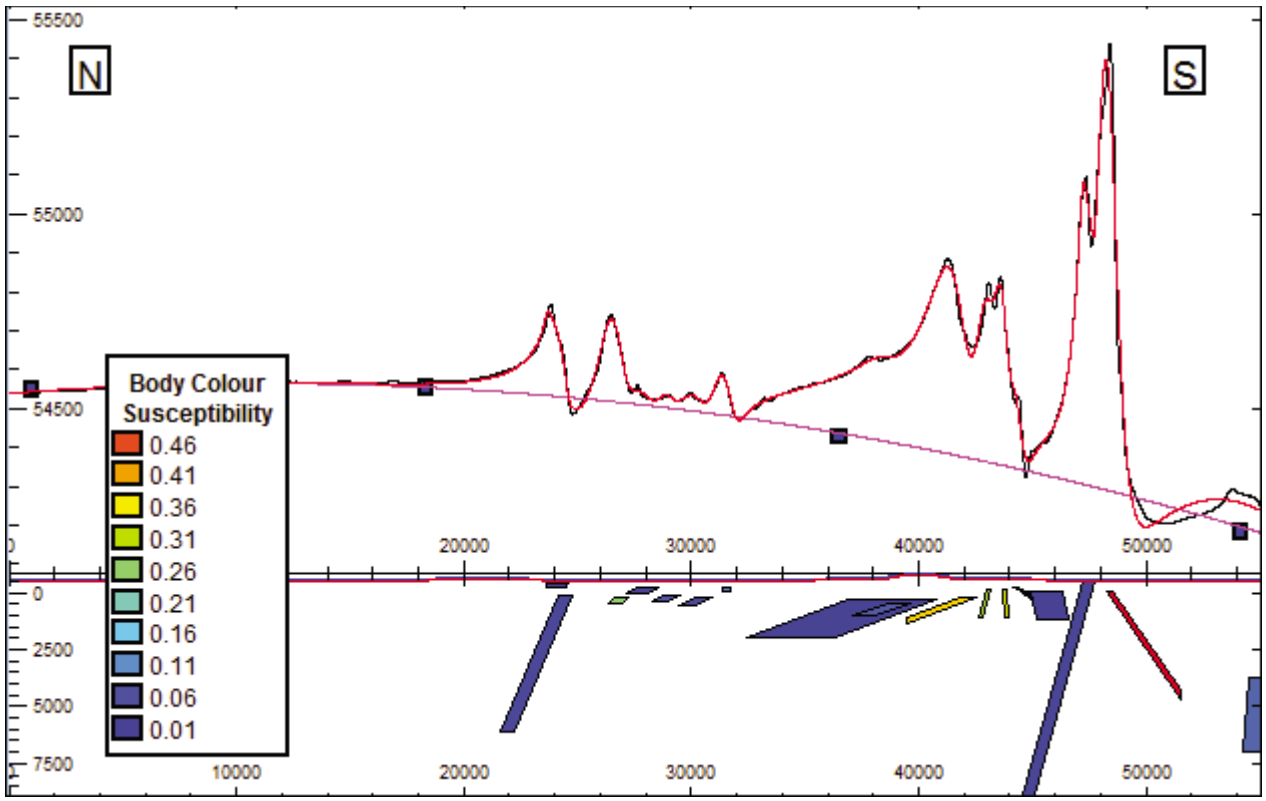

Figure 15. Southern margin example north-south aeromagnetic profile with source model. Magnetic susceptibilities are in SI.The location of the line is show in Figure 14.

3.2 Magnetic field mapping of the northern basin margin

The vertical derivative of TMI over the northern basin margin is shown in Figure 16. The northern margin of the basin is more clearly defined in the magnetic field imagery than is the south, with an abrupt and simple limit of the sharp, high amplitude magnetic field variations over the southern margin of the Arunta Block. There are two areas of subdued magnetic signature to the north of this margin, that appear to be due to a cover of sedimentary rocks in what may be broad but shallow basins perched on the Arunta Block. In many places the basement magnetic signature around these zones can be traced considerable distances, as the magnetic sources plunge gradually beneath the cover. The western margin of the Arunta Block is marked by high amplitude magnetic anomalies truncated irregularly against a southwest-northeast trending zone of what appear to be shear structures. In several places immediately to the south of the southern margin of the Arunta Block, there are smooth, moderate to high amplitude anomalies, which appear to be the same highly magnetised rocks downthrown to the south across vertical or steep basin bounding faults.

The vertical derivative of Bouguer gravity over the northern basin margin is imaged in Figure 17. Unfortunately, the Central Petroleum airborne gravity survey does not extend over the basin margin, but this area is covered with a high density of ground stations. The basin bounding fault interpreted from the clearly down-thrown magnetic basement directly south of the southern edge of the Arunta Block has a surprisingly subdued gravity signature, suggesting that there may be only a slight density contrast between these basement rocks and the Amadeus basin sediments. The southwest-northeast trending western margin of the Arunta Block interpreted as due to shear structures in the magnetic field imagery is also clearly evident in the gravity data, suggesting that this is a major crustal structure.

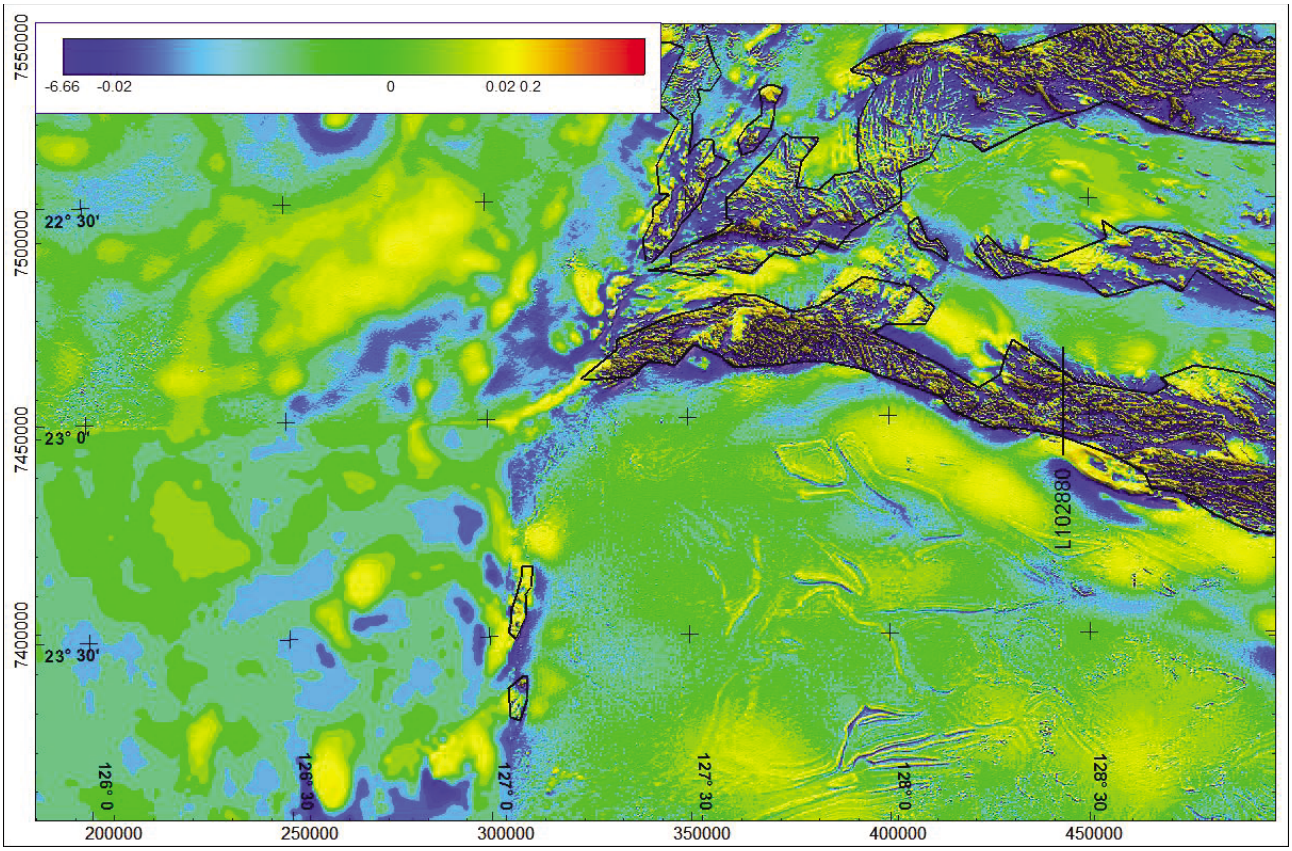

Figure 16. Northern margin vertical derivative of TMI. Units are nT/m.

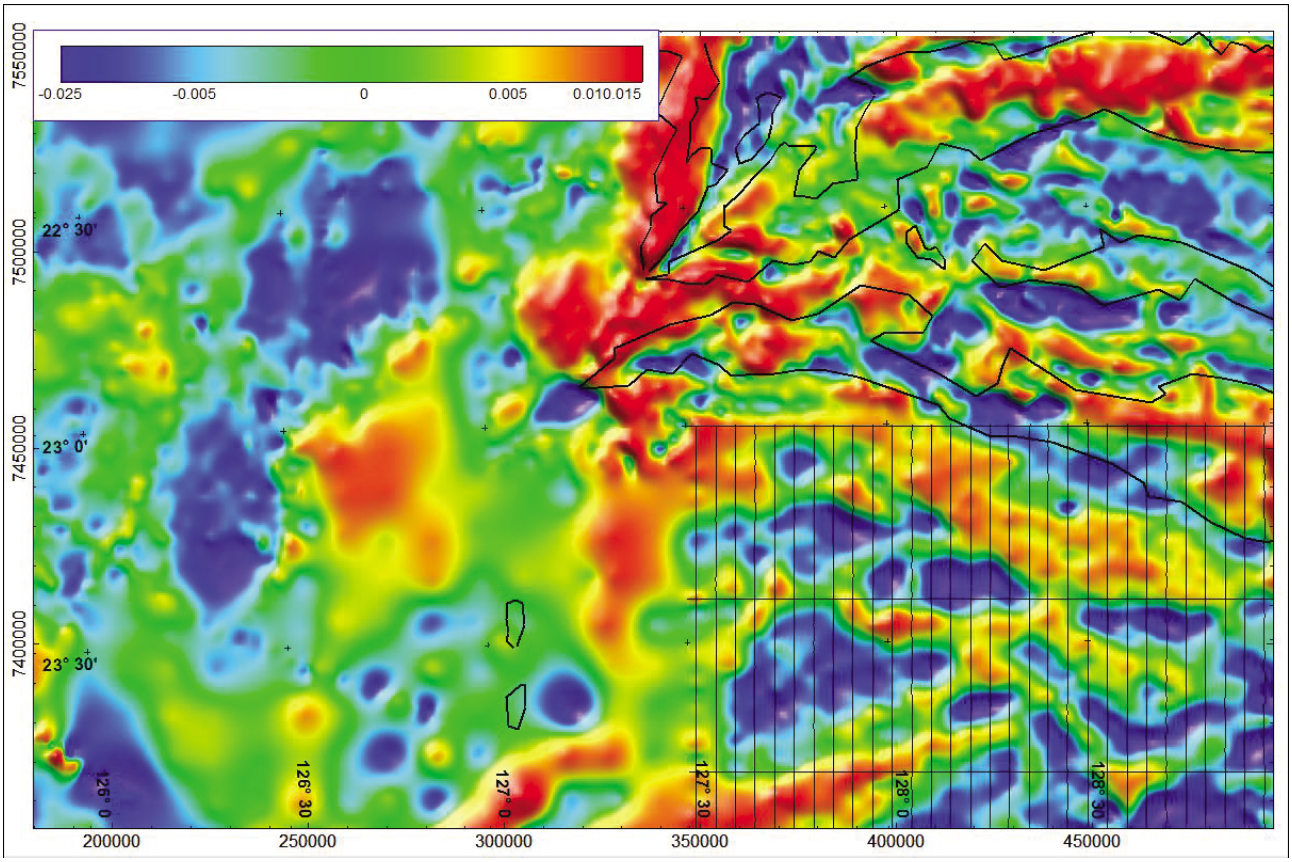

Figure 17. Northern margin vertical derivative of Bouguer gravity with Central Petroleum airborne gravity survey flight-lines. Units are Eotvos x 10^{-3}.

The gravity mapping from the closely spaced stations over the Arunta Block reveals clear linear, low amplitude features. These are interpreted as limited-relief block faulting beneath what have been interpreted as perched basins on the Arunta Block basement (in many cases these are not basin-bounding faults, because as described from the magnetic field image, the sedimentary cover appears mostly to on-lap gradually onto the basement). Conversely, the lack of clear gravity definition of structure immediately to the west of the Central Petroleum survey area, and to the south and west of the Arunta Block, is most probably a limitation of the sparse gravity station coverage in that area. This is unfortunate, as it should be a critical area for understanding the relationship between the Amadeus Basin, the eastern Canning Basin to the west, and the major southwest-northeast trending structure at the western margin of the Arunta Block.

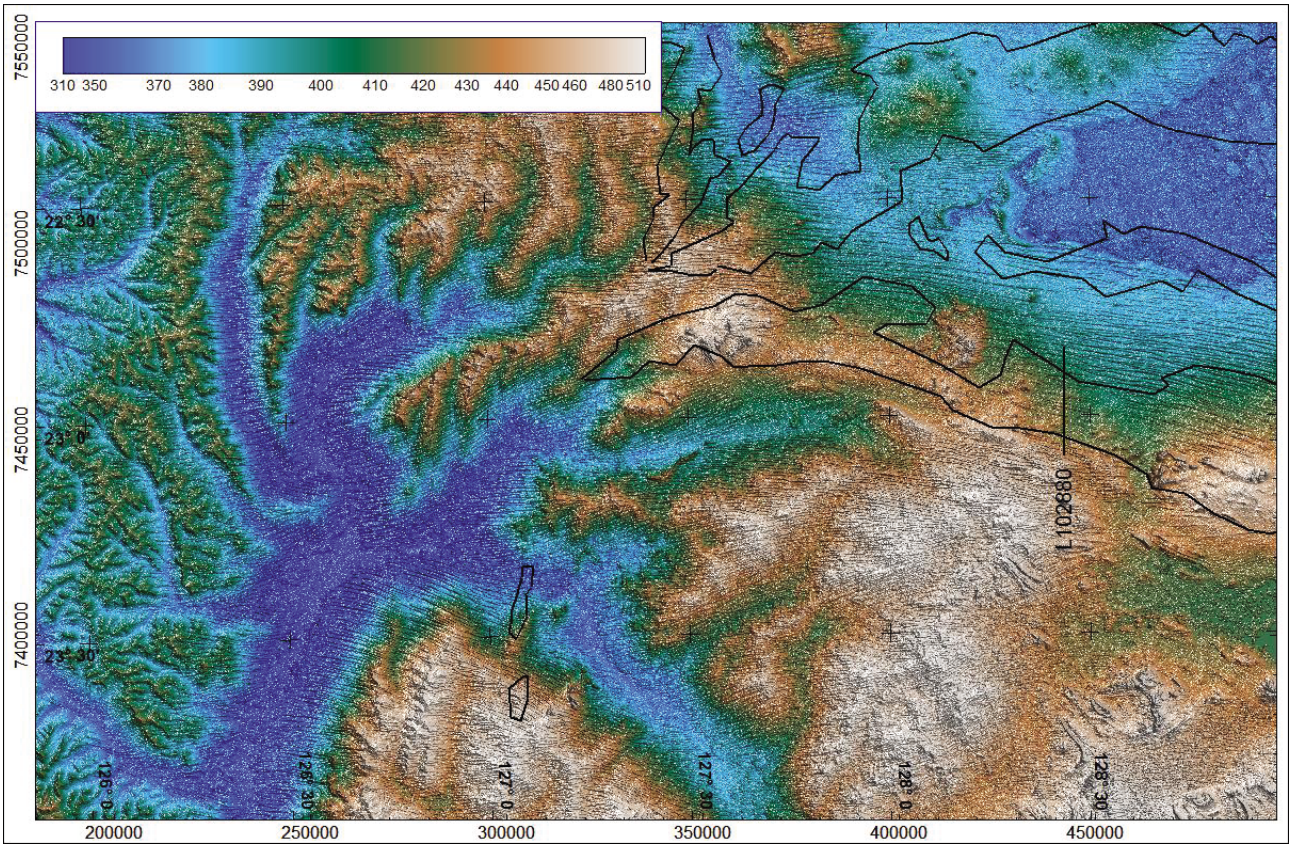

Figure 18. Digital terrain Model over the northern basin margin. Unit – elevation above sea level in metres.

The digital terrain data shown in Figure 18 provides little assistance in locating the northern margin of the Amadeus Basin. Some of the structure in the basin itself has topographic expression, but the Arunta Block is mostly covered by sand dunes, and the salt pans of Lake Mackay, with only a little sharp relief at separated locations along the southern margin of the Arunta Block providing opportunity for bedrock outcrop. The scarcity of bedrock outcrop is evident in the 1:250,000 Webb geological sheet shown in Figure 19, and it is clear that the gravity and magnetic data have a key role in helping to reveal the geological structure across this sheet.

Figure 20 shows a modelled north-south flight-line over the northern margin of the Amadeus Basin. On this line, the southern margin of the Arunta Block is marked by a high amplitude (ca. 1000 nT) sharp magnetic anomaly, modelled as due to a thin, high susceptibility (0.08 SI) body steeply dipping to the south. The smooth magnetic high over the Amadeus Basin at the southern end of the line is modelled as due to a source at about 4 km depth. Many of the magnetic sources to the north are at depths of only a few hundred metres. Interpretation of the magnetisations to depths of about one kilometre is uncertain, as these may be overlain by weakly magnetic sediments, or they may simply be areas where the shallow basement rocks are only weakly magnetic.

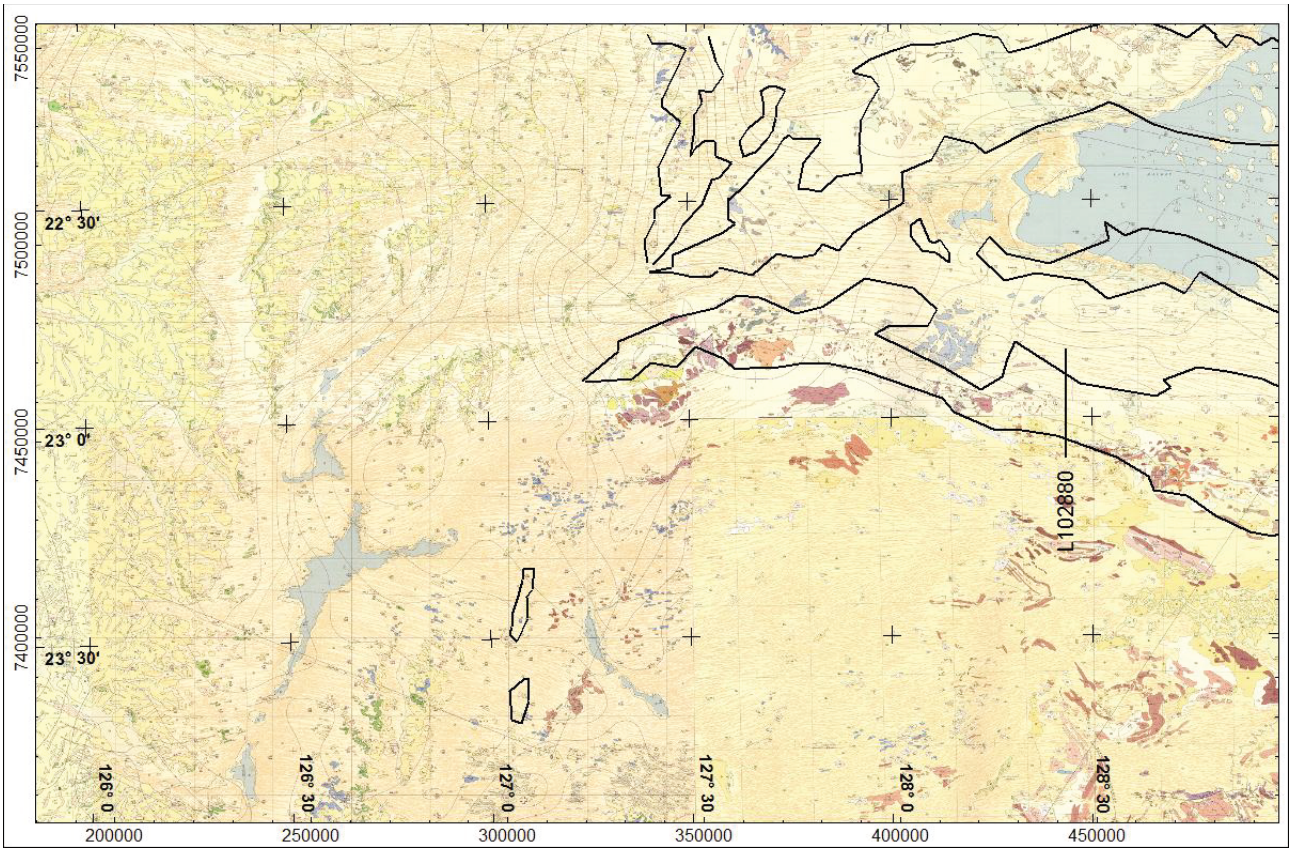

Figure 19. Northern margin interpreted from magnetic data over a merge of the Webb, Wilson, Ryan and Macdonald 1:250,000 geological maps.

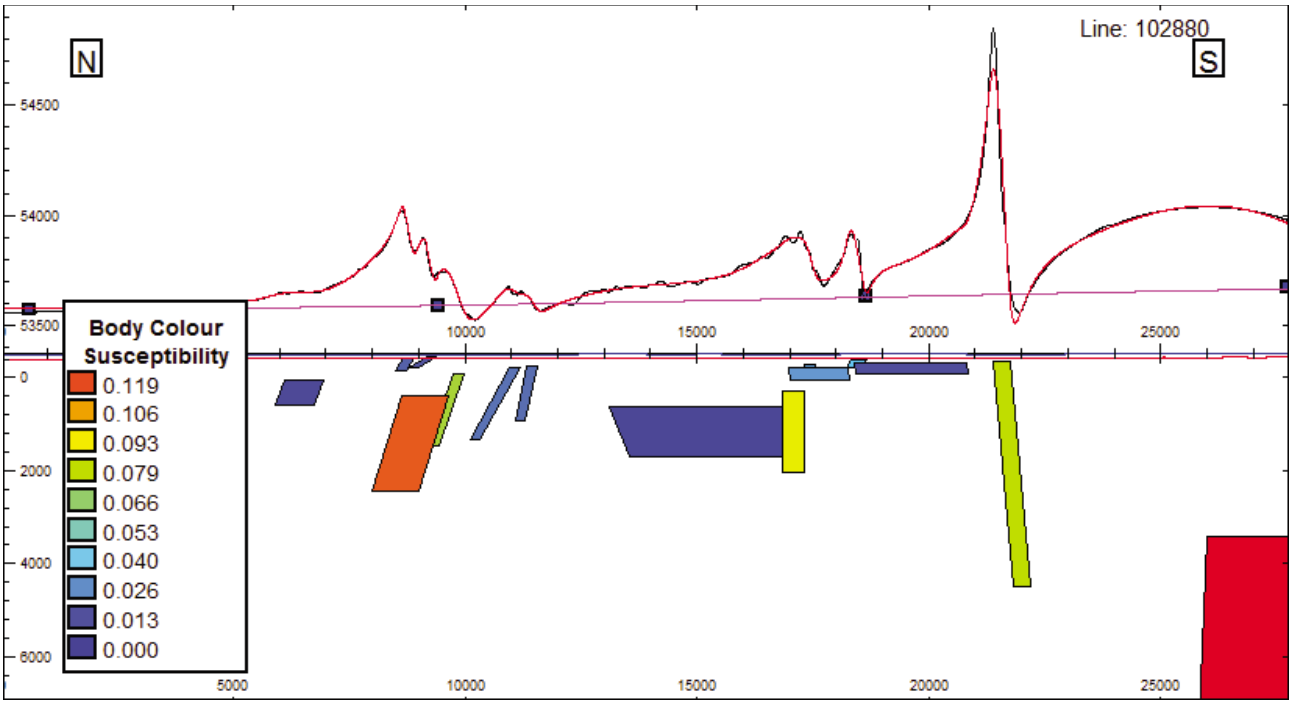

Figure 20. Northern margin example north-south aeromagnetic profile with modelled source bodies (line located in Figure 19). Susceptibility units in SI. The black trace is measured TMI, the purple trace is the assumed background field, and the red trace is the model computed field.

4 MAGNETIC SOURCE DEPTH MODELLING

Generally only igneous and metamorphic rocks have magnetisations of sufficient strength to give rise to readily detectable aeromagnetic anomalies from sources at depths in excess of several hundred metres. For no basin as large as the Amadeus, does the magnetic field variation match that of an excavated material of homogeneous magnetisation. Rather, the magnetic field variations are dominated (as they are over areas of basement outcrop) by lateral variation in basement magnetisation, modulated by the basin only in the variable smoothing, attenuation and filtering of the field according to lateral variations in basin depth. Magnetic field interpretation can only be used where well resolved anomalies provide spot estimates of depth to the top of a magnetisation. The general expectation is that those magnetisations extend to the basement surface, where they are truncated by an essentially horizontal unconformity, and thereby that those are estimates of the local depth of the basement surface. At even shallow depths, the detailed internal distribution of magnetisation in a small to moderate size body is generally of little importance, as it can be well represented by a homogeneous magnetisation. The inverse problem of mapping a magnetisation from its magnetic field expression is inherently non-unique. In particular, it is always possible to find a distribution of magnetisation to match a measured magnetic field at any depth shallower than the true source depth. However, with only a few simple assumptions, such as that the magnetisation is homogeneous, compact, and bounded by sharp, flat sides and a horizontal top (i.e. that it forms a tabular body) it is possible to find a single best-fit body to explain that magnetisation. The model sensitivity of the estimated depth is at very best of the order of ± 5%, but more generally may be ± 10% to ± 15%. There is also additional uncertainty in assigning a geological representation to any model. This problem arises where there may be thick volcanic units above basement, but this is not believed to be a concern in the Amadeus Basin. One principal limitation of estimating depth from magnetic field data is that this is possible only at the location of suitable anomalies. Over large parts of the Amadeus Basin, the sedimentary rock thicknesses are so large, or the basement magnetisations are so weak, that there are no detected anomalies in the magnetic field from which to estimate a source depth. In some parts of the Amadeus Basin, detection of magnetic signal from the basement surface is made more difficult by a cover of weaker but much shallower magnetisations. These magnetisations, variably sourced by maghemite in surface drainage and palaeo-drainage systems, and by weak formation magnetisations within the shallow Amadeus Basin sedimentary rocks, generate short wavelength field variations which either mask weak signals from stronger but much deeper basement magnetisations, or reduce the precision with which those basement signals can be matched, increasing uncertainty in the estimated depths.

The process of estimating magnetic source depth is illustrated in Figure 21. A suitable anomaly from which to estimate a depth is located, and a traverse is drawn through the anomaly, passing through the anomaly peak and trough, parallel to the steepest gradients. The background field variation along that traverse is estimated as a smooth curve, asymptotic to the background field away from the anomaly. A flat-topped, tabular source model is located beneath the anomaly, and the trend and strike length are adjusted to approximately match those of the anomaly. Then the best-fit set of parameters (depth to top, thickness, magnetic susceptibility, and plunge and depth extent) are simultaneously solved for in an iterative, multi-parameter inversion. This inversion provides the estimated depth to the top of the magnetisation, together with values for the other parameters which may be diagnostic of the source geology.

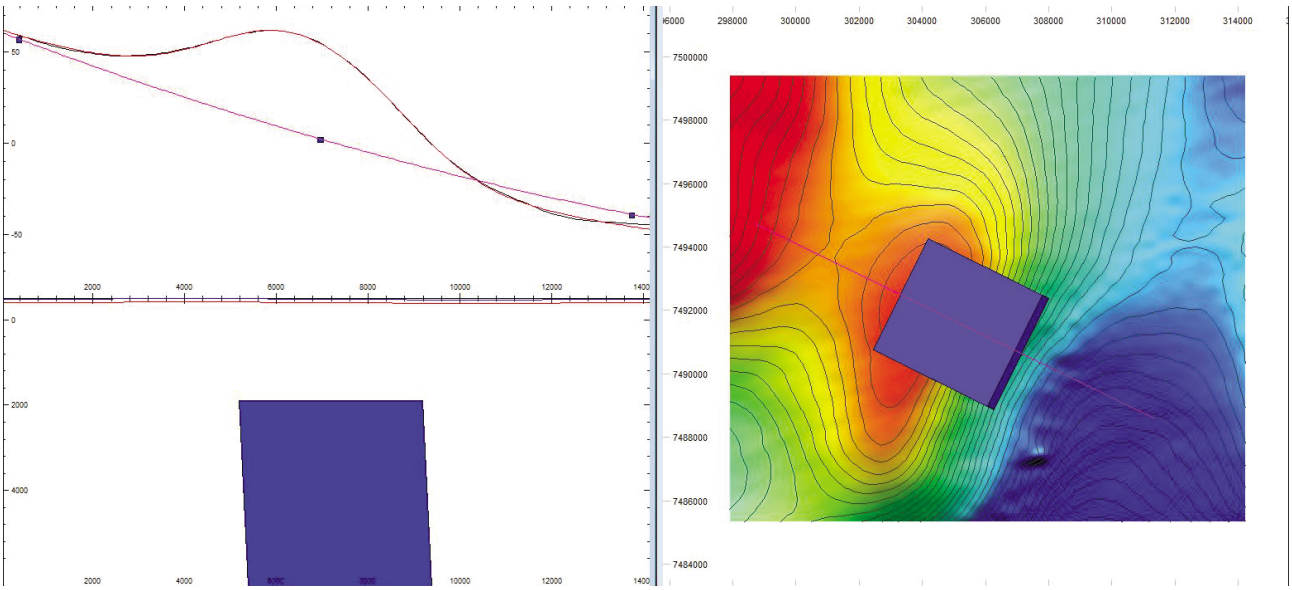

Figure 21. Example magnetic modelled depth to source section (left) and location of section over TMI image (right). The black trace is the measured TMI, purple is the interpreted background field, and red is the model computed field summed with the background field.

This process of depth estimation, which is user-controlled at all stages, outperforms automated methods. However, estimation of source depth from magnetic field data, by any method, is the solution of an inherently non-unique inverse problem, requiring either explicit or implicit assumptions about source characteristics. In this application, the assumptions appear to be well justified. In particular, the flat top of the sources is consistent with the geological expectation that these are samples of a locally horizontal unconformity surface, and the substantial depth to these sources relaxes any requirement that they are internally homogeneous. The principal source of uncertainty in the depth values arises from the ability for an error in that parameter to be effectively compensated by a suitable combination of errors in the other parameters. The highest feasible sensitivity to model depth is ± 5%, but more realistic uncertainties on the depth values are of the order of 15% for the population of solutions, with higher uncertainties and errors likely on some individual values (particularly the deeper ones). There is little support for substantial volcanics or intrusives into the Amadeus Basin section. Therefore depths are unlikely to be derived from sources above the base unconformity, but there is also the possibility that some sources are emplaced beneath the base unconformity, so that depths derived from those sources lead to overestimation of basin depth.

The mapped distribution of depth solutions is plotted in Figure 22, with solutions colour and size coded for depth. The dark blue solutions (depths <2000 m) mostly occur around the basin margins, and along the interpreted junction between the Canning and Amadeus Basins. Many of the depth solutions over the northern half of the Amadeus Basin are in the range of 4 to 6 km, with higher values of 8 to 12 km over the central part of the basin. Depths over the Canning Basin are less, with many depths in the range of 3 to 7 km. The model source bodies themselves are plotted in Figure 23a. The bodies have been colour coded according to their provenance. The green models are shallow sources close to the basin margins (light green solutions over the Musgrave Block, and dark green solutions over the Arunta Block). The red bodies are those beneath the Amadeus Basin, which can be seen to be deeper over the south and centre of the basin, stepping up to shallower depths towards the north. Bodies beneath the Canning basin (coloured blue in Figure 23a) are mostly shallower than those beneath the Amadeus Basin. The north-south trending line of shallow sources between the Amadeus and Canning basins (shown in purple in Figure 23a) are mostly of small volume, are considerably shallower than those to the east or west, and are not associated with a substantial gravity high, as would be expected for a basement high. A shaded greyscale surface of the magnetic source depth model is shown in Figure 23b.

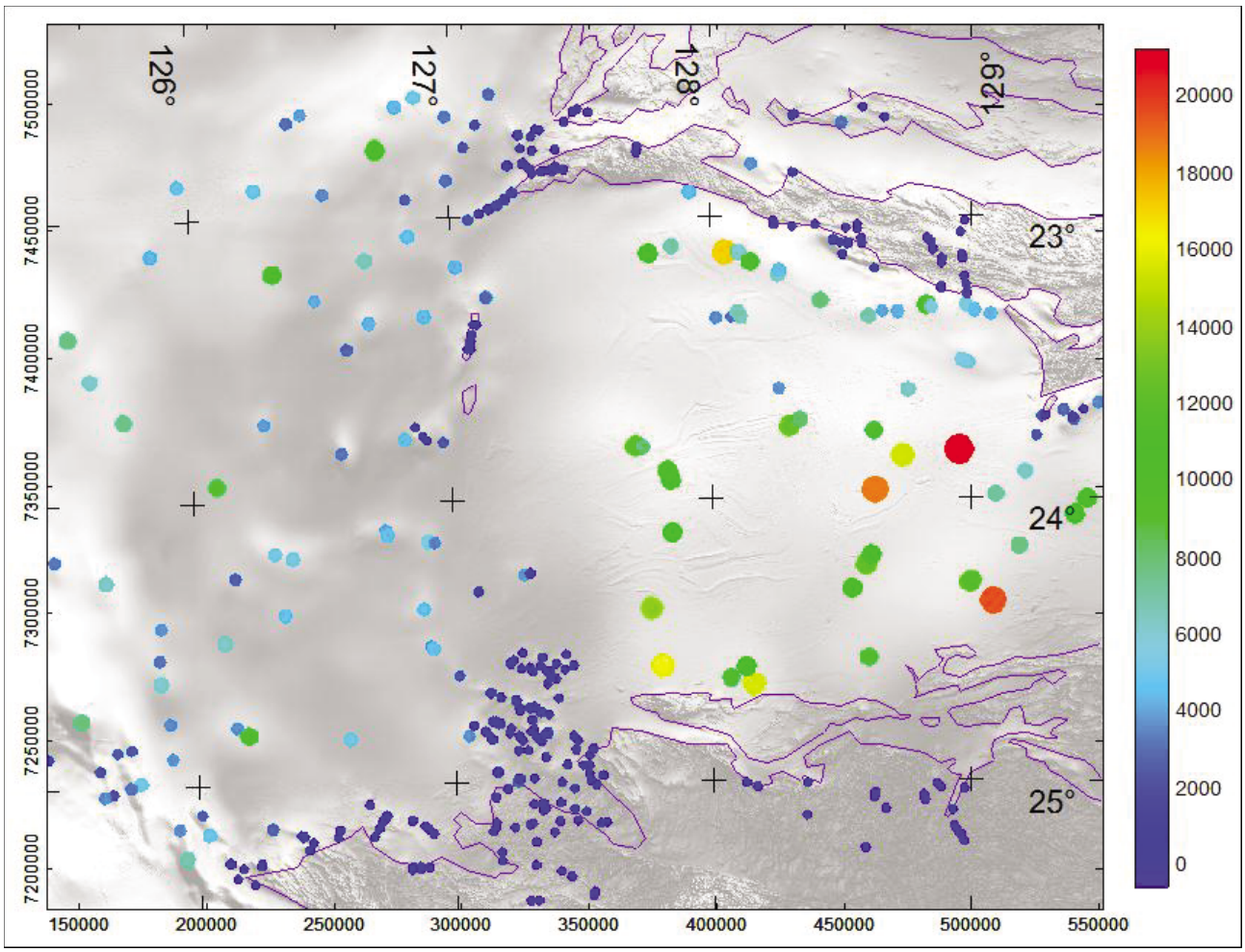

Figure 22. Magnetic source depth (colour scale depth in metres) solutions over a greyscale TMI image.

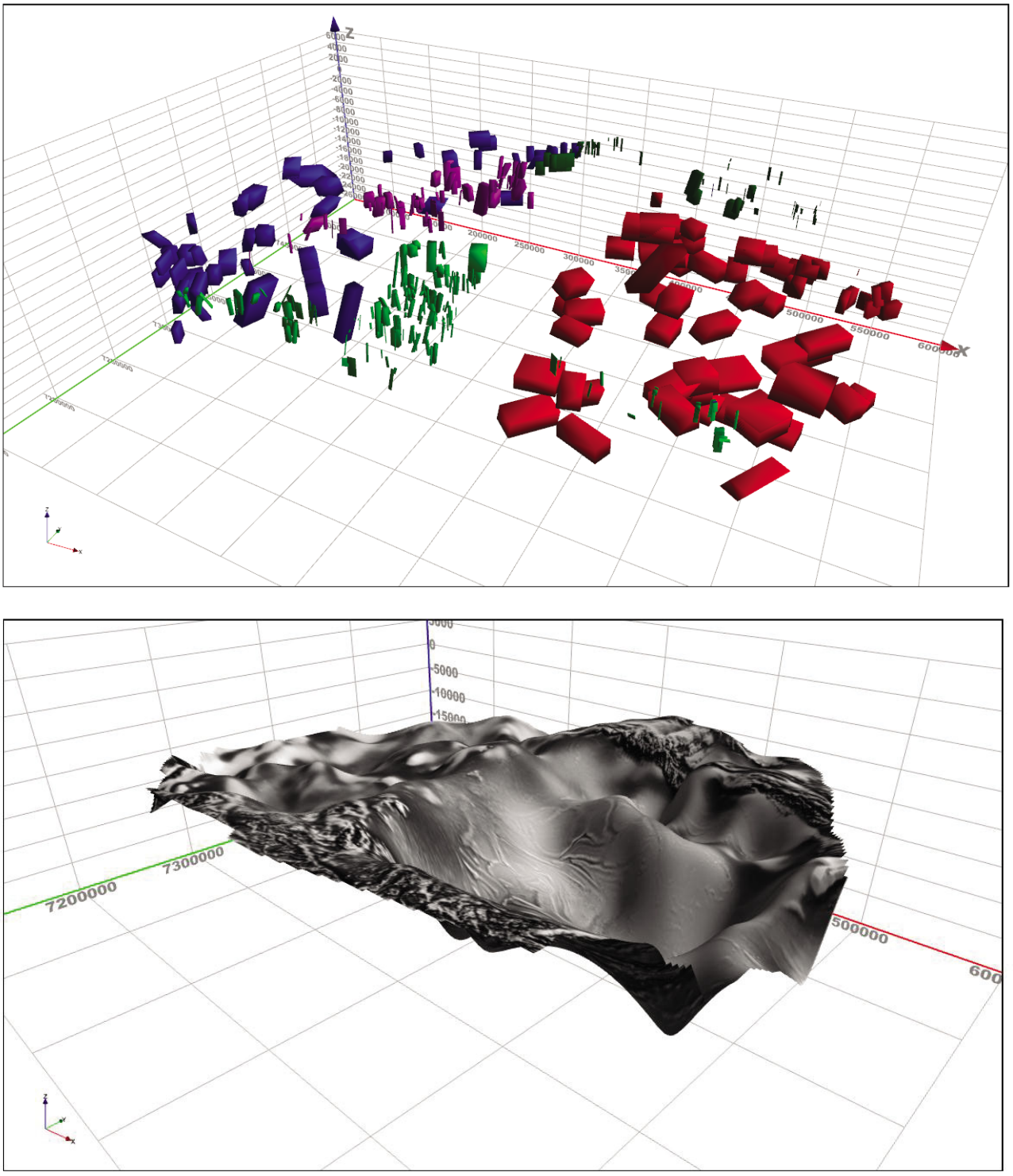

Figure 23. a) (top) Magnetic source models. Red - beneath the Amadeus, light green – Musgrave Block, dark green – Arunta Block, blue - beneath the Canning Basin, and purple - at the interface between the Canning and Amadeus basins, b) (bottom) grey shaded top surface of magnetic source depth model. Both figures viewed looking from the southeast of the study area towards the northwest.

5 GRAVITY MODELLING

5.1 Modelling concepts

It is not feasible, particularly with the very limited constraints available, to derive a meaningful structural model of the basin from any un-guided inversion of the gravity data by itself. Rather, it is necessary to propose one or more feasible basin structural models as the basis from which to invert and interpret the gravity data. The gravity coverage across the basin can be considered as a single constraint surface (weak in those areas of sharp variation which are poorly sampled). From that constraint, it would be possible to define a single density contrast interface, if topography of that surface was the sole cause of gravity variation, and if the density-contrast value, and one or more control points were known. The challenge of the interpretation is that, as listed in section 2.1, there are at least four categories of cause of variation in the mapped gravity across the basin, all of which are expected to contribute significantly to the observed gravity variation over at least some parts of the basin, with no reliable grounds for discrimination between them. The problem is not of finding a model which is capable of matching the observed gravity variation, but of justifying that model as a reasonable selection from all available models which could fit the data. Given the wide range of possible alternative models, it is indeed very unlikely that any selected model derived from gravity inversion is a close representation of the true basin structure. It would be a massive undertaking (and of little practical value) to attempt to derive an atlas representing the range of all possible models. Instead, the present model is presented as one feasible solution, which is hopefully useful as a support for geological speculation and hypothesis. The model is available in digital format, as a resource to be adapted to test alternative geological hypotheses, and most importantly, to be changed as new constraints become available from future studies. The following considerations are noted with regard to major expected causes of gravity variation across the basin.

5.1.1 VARIATION IN BASEMENT DEPTH, WITH A DENSITY CONTRAST BETWEEN THE BASIN FILL AND THE UNDERLYING BASEMENT

Increase in basement depth beneath a lower density sedimentary section is the classic explanation of negative gravity anomalies over sedimentary basins. It is most appropriate for shallow, small basins developed over a much denser basement. According to this model, the deepest depo-centres of the basin are at or close to the gravity minima, and in areas of gradual gravity variation it should be possible to use gravity contours as a proxy for basin depth. Such a simplistic model is manifestly insufficient and inappropriate to derive a realistic model of the Amadeus basin from the gravity data. Basement depth has been imposed on the model where feasible, as suggested by the magnetic source depth modelling. Those source depths may in the best circumstances be reliable to within 15%, and more substantial error and uncertainty arises if the top of those magnetic sources is not in fact the top of basement. It was considered unlikely that magnetic source depths in excess of about 10 km, away from regional gravity minima, record such considerable depths of Amadeus Basin sedimentary rocks. Pre-Amadeus Basin sedimentary rocks, possibly developed locally in earlier rift centres, may account for the difference between depth to the magnetic basement, and the thickness of the Amadeus Basin section.

5.1.2 LATERAL VARIATION IN DENSITY OF THE BASEMENT ROCKS

Even a cursory inspection of the gravity imagery across the Arunta and Musgrave Blocks, bordering the Amadeus Basin, reveals considerable lateral variation in gravity over regions of consistent basement depth, due to variation in density between units of different basement lithology. Mafic intrusives (extensive within the Musgrave Block) may have densities well over 3 gm/cc, and granites or acid gneisses composed essentially of quartz and feldspar have densities as low as 2.67 gm/cc, providing the basis for relative density variations in excess of 0.5 gm/cc. The large area of these basement units, and their considerable depth, constitute huge volumes, which readily generate gravity variations of

hundreds of μmetres/s^2 (tens of mGals), a range of more than 50% of the observed gravity variation over the basin. While it is most likely that such density variations occur within the basement beneath the Amadeus Basin, there are very few grounds for mapping those variations. In some cases gravity highs over the surrounding basement are associated with magnetic anomalies. These examples include some of the Giles intrusions of the Musgrave Block, but in many cases the magnetic anomalies are due to extreme magnetisation intensities within relatively thin units, without the volume to cause substantial gravity variation. There is no clear evidence that the deep bodies generating magnetic anomalies over the basin are high density, and so they were not used in the gravity modelling, other than for supplying estimates of basement depth. The gravity model has been derived with a constant basement density of 2.8 gm/cc, which is considered a reasonable representation for the range of lithologies expected to constitute most of that basement. Subdivision of the basement into different density units should only be performed if and where there is direct justification for such subdivisions.

5.1.3 VARIATION IN DENSITY OF THE INFILLING SEDIMENTS (PARTICULARLY BETWEEN HALITE-DOMINATED FORMATIONS AND SANDSTONE-SHALE, OR CARBONATE DOMINATED FORMATIONS

The role of salt in the gravity expression of the Amadeus Basin is problematic. There is widespread outcrop evidence for salt, intersection of salt in boreholes, recognition of salt in seismic sections, and substantial areas across which outcrop patterns are interpreted as the expression of salt tectonics or of deformation influenced by the mobility of salt, but the sum of this information is far from sufficient to evaluate the gravity expression of salt over the basin. The density of halite is approximately 2.2 gm/cc, and the density of anhydrite is approximately 3.0 gm/cc. A density of 2.5 gm/cc was assumed for the undifferentiated basin sediments. Replacing a section of the unassigned basin infill with halite, with double the density contrast against basement, produces a similar gravity expression from a halite unit of only half that thickness. The effect of replacing a 1 km section of the 2.5 gm/cc model unit with a halite unit of 2.2 gm/cc would be to reduce the gravity values over that section by 120 μm/s^2. It would however require only about one part anhydrite to two parts halite in an evaporite formation to have a neutral contrast against the undifferentiated formation density of 2.5 gm/cc.

The principal strength of the gravity method is in detection and delineation of steeply dipping density contrasts. A buried horizontal salt layer with tapered margins would have no diagnostic expression in the gravity data, although it locally reduces the value of gravity, mimicking a more substantial depression of basement beneath standard density sedimentary rocks. Salt has a prominent expression in gravity data where it is mobilised in sub-vertical structures. There are a few sharp, circular gravity lows in the Amadeus Basin that might indicate salt domes, but more commonly, in some areas where the gravity field is well resolved by a high density of measurements, there are sharp linear gravity lows, which might be due either to low density sedimentary rocks between two horst blocks of denser basement rocks, or to salt walls, where the salt has been mobilised along a linear fault or basement step. Salt units have not been included in the model, although they clearly exist, principally because of the lack of constraints. This is not a major drawback to the model, as, if and when better constraints become available, it is possible to introduce a salt unit into the undifferentiated basin fill, with minor and local subsequent readjustment of the underlying basement surface.

5.1.4 VARIATION IN CRUSTAL THICKNESS ACROSS THE BASIN.

The Amadeus Basin may have developed initially as a broad region of crustal extension, possibly including localised rift development, in response to regional heating, and subsequent thermal relaxation and crustal thinning. Such patterns are recognised world-wide across many major rifts, and provide a feasible mechanism to deposit substantial thicknesses of sediment onto what would otherwise be buoyant continental crust. It should be expected that initial development of the basin would have involved: 1) thinning of a continental basement (of unknown original thickness) - with more extreme local thinning beneath specific rift zones, and 2) with a subsequent sag phase involving the major basin development - with a largely consistent stratigraphy over a very wide area. For the Amadeus Basin this basin structure has been substantially modified in a series of orogenic events. These modifications include inversion by compressive forces with: 1) subsequently steep dip of the basin section in some marginal areas, and 2) possible vertical displacement

of basement blocks beneath the basin. If this hypothesis is correct, some of the gravity variation across the Amadeus Basin is likely to be due to topography on the base of the crust. However, with no reliable independent constraints, the base of the crust has been kept as a horizontal surface in the present gravity model. The consequence of any substantial crustal thinning beneath the basin (with an associated increase in gravity) would be to require a corresponding increase in sediment thickness within the basin (or a decrease in assigned basin infill density) to compensate.

5.2 Density values used in the modelling

A key feature of the model is the relative density values assigned to the different model units. Exact values for these densities are not known, but error in assigning representative values to specified model units are likely to be less significant than errors in incorrectly assigning (or in omitting) model units – specifically, any thick halite-dominated sections, and any substantial local variations in basement density. The Amadeus and Canning Basin formations have both been given bulk, homogeneous values of 2.5 gm/cc. This value appears reasonable for moderate to low porosity clastic sediments. Higher densities should be used for any carbonate units, and lower densities for substantial anhydrite-poor salt formations. The age of the Amadeus Basin sedimentary rocks, and the fact that substantial sediment thicknesses may have been removed above the present level of exposure, means that there is not necessarily a large density gradient with depth, as is common in younger basins.

The basement density of 2.8 gm/cc is similarly a compromise value to represent rocks which will almost certainly have a range of densities, possibly between 2.7 and over 3 gm/cc. The most critical factor for the modelling is not the absolute values used, but their relative contrasts. The contrast between assigned basin and basement densities is 0.3 gm/cc. Basement depths would have to be varied in inverse ratio to any change in this contrast (so that a halving of the contrast to 0.15 gm/cc would require an approximate doubling of the basin depth). Unknown lateral variation in basement density is one of the major concerns in validity of the model. Density variation within the basin infill package is likely to have predominantly horizontal layering at the basin scale, despite the evident presence of large scale folding. However, lateral variations in basement density across steeply dipping intra-basement contacts is likely to have a more profound influence on the model.

5.3 Construction of the model

In view of the substantial uncertainties involved, there is no justification in generating a detailed three dimensional model of the basin, with apparent high resolution, but very high uncertainty. Rather, a coarse, simple model has been generated, with detail kept to the minimum required to match the measured gravity variation, using guidance of the depths estimated from the magnetic field interpretation. The model was generated on a set of 8 north-south traverses, at 50 km spacing, consisting of 50 km wide blocks, with step discontinuities between the blocks. The gravity field is simultaneously computed on all traverses, from all of the model blocks, to generate a full, although coarse, 3-D model of the western section of the basin. The north-south traverse direction was selected as being perpendicular to the main gravity field variations. In order to reduce the iterative adjustment of the model, as it is generated line by line, an initial strike model was created on three east-west traverses, and the intersections of that model on the subsequent north-south traverses was used to digitise a starting model which already approximately fits the data. The location of both the east-west and north-south model traverses is shown in Figure 24.

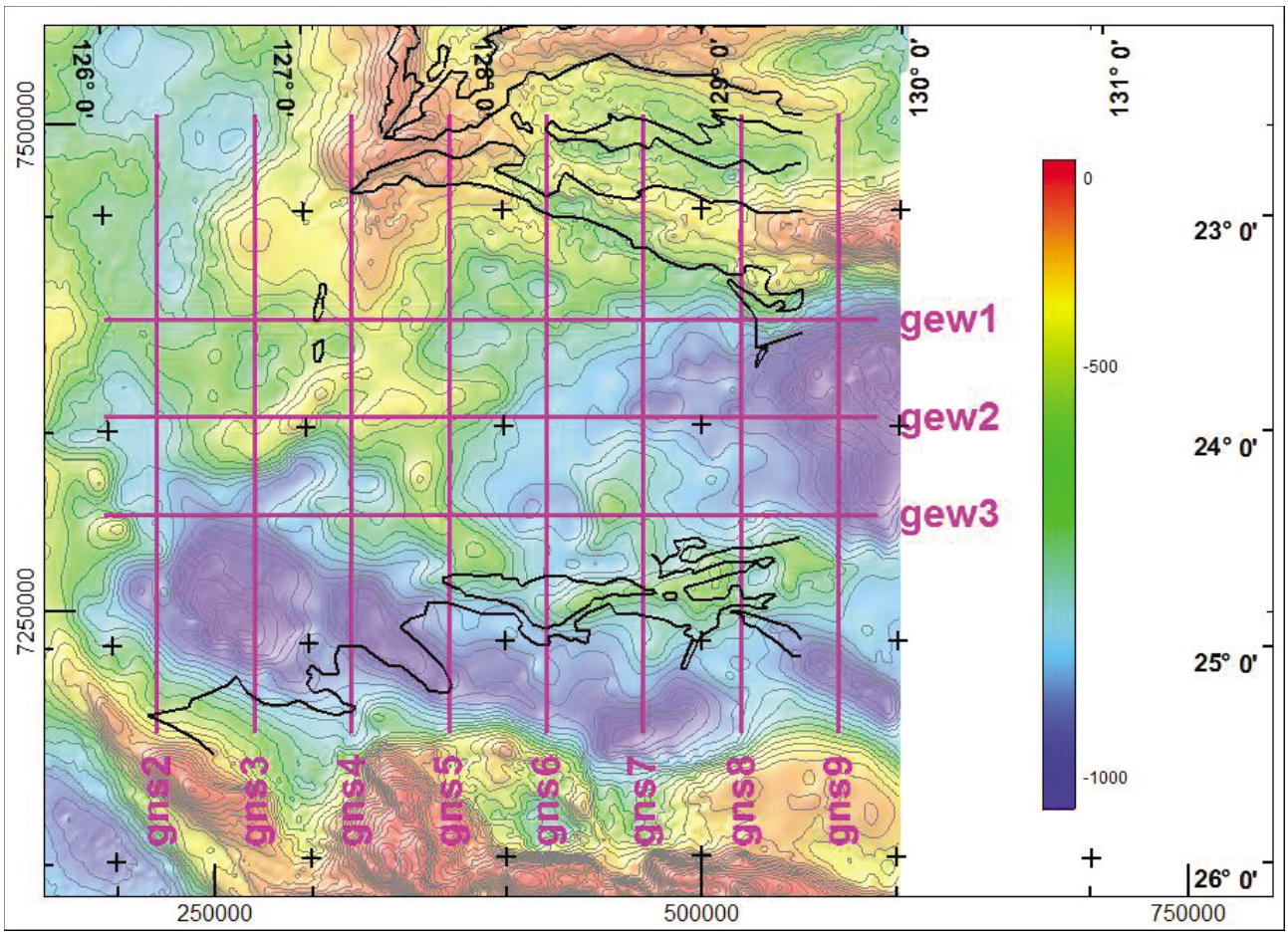

Figure 24. Distribution of the gravity model sections.

Figure 25 shows the northernmost of the 3 east-west model sections. The Bouguer gravity variation is subdued, with a total range of only 300 µm/s^2 across the Canning and Amadeus basins. The shorter wavelength variations of about 20 km wavelength can most easily be explained as due to topography of the basement interface, or lateral density variations in the basin section or in the basement immediately beneath the basin. The broader variation of up to 200 km wavelength is most easily modelled as due to variation in basement depth (as has been done here), or could equally well be modelled as due to variation in crustal thickness beneath the basin. The decrease of gravity over the Arunta Block at the eastern end of the line is of uncertain significance, as this line is oblique to the main gradient and the basin margin. Intersections with the magnetic source models derived from the magnetic depth estimation study are shown in red. These bodies were used to guide development of the gravity model, but were not assigned densities, so do not contribute directly to the gravity model.

Figure 26 shows the middle of the three east-west model lines, parallel to that of Figure 25, and 50 km to the south. A major feature to be explained in this profile is that the magnetic source depth models suggest a considerable deepening of the basin, across a section for which the gravity data has a consistent, low gradient. This apparent difference between the gravity and magnetic fields is explained by introducing a section of (non-magnetic) sediments or meta-sedimentary rocks beneath the Amadeus Basin section, which has a reduced density contrast against the underlying basement. An alternative explanation is that the tops of the deeper magnetic sources are not part of a basement interface.

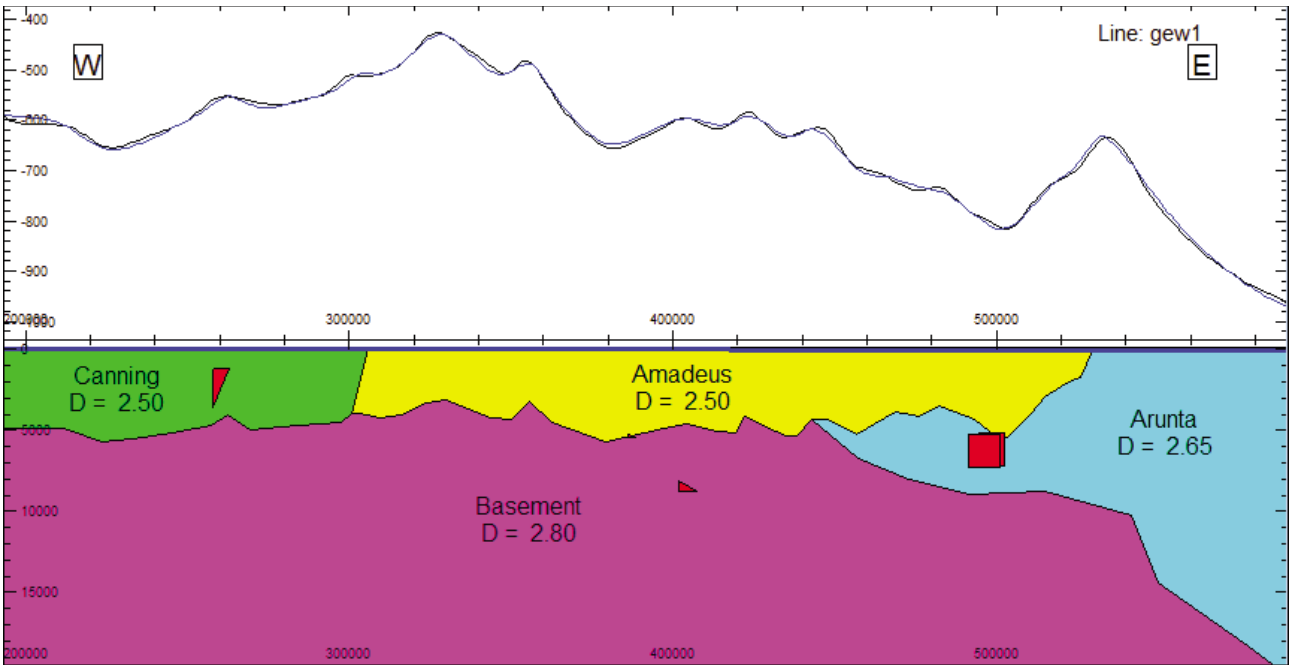

Figure 25. Northernmost of the 3 east-west gravity model sections, Gew_1.

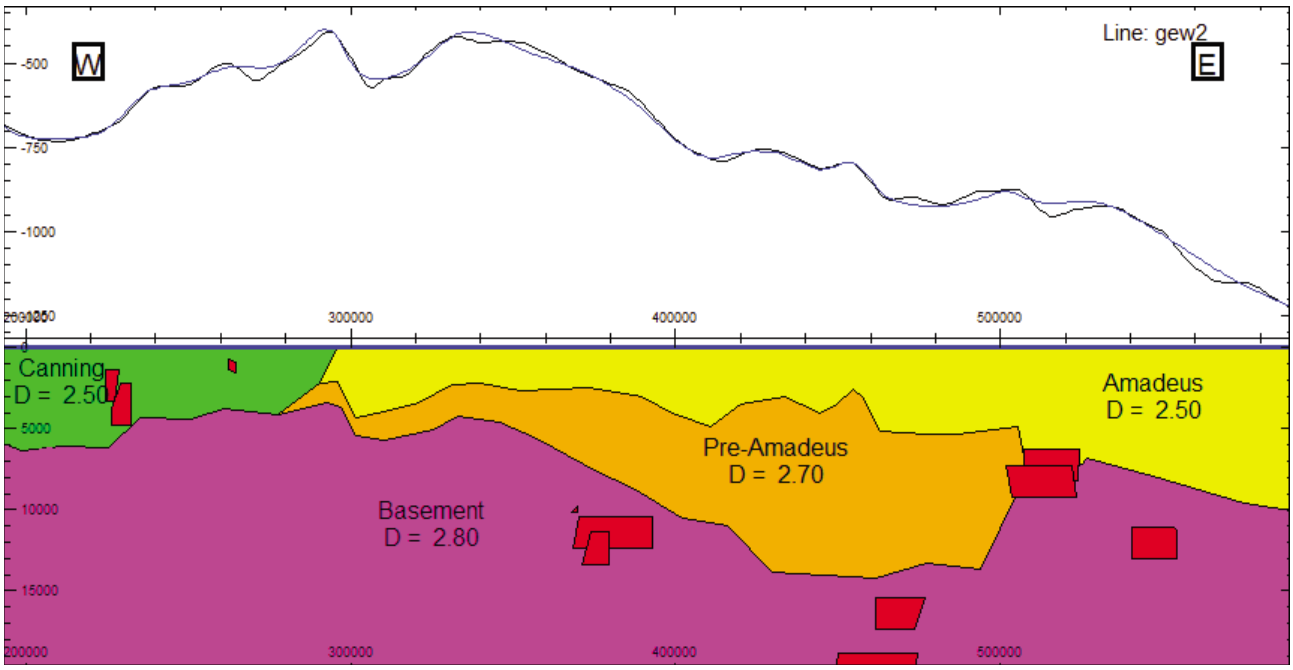

Figure 26. Central east-west gravity model section, Gew_2.

Figure 27 shows the southernmost of the three east-west profiles. There is a very irregular gravity variation, with a net decrease in gravity of 500 µm/s^2 from west to east. This is modelled as due to a deepening of crystalline basement. The magnetic source depths in excess of 10 km along this profile also appear too deep to be easily explained as marking a basement surface immediately beneath the main Amadeus Basin section (for instance with the Heavitree/Dean Quartzite as the basal unit). Instead, these sources have also been modelled as marking an earlier basement surface beneath a thick pre-Amadeus Basin section. The abrupt changes in gravity along this section are best explained as due to block faulting. While that block faulting must disrupt the top of crystalline basement, because of the sharpness of the gravity variations, and the requirement to peg the top of basement at the magnetic source depths, the major cause of the gravity variation has been modelled as due to faulted relief on the top of the pre-Amadeus Basin section.

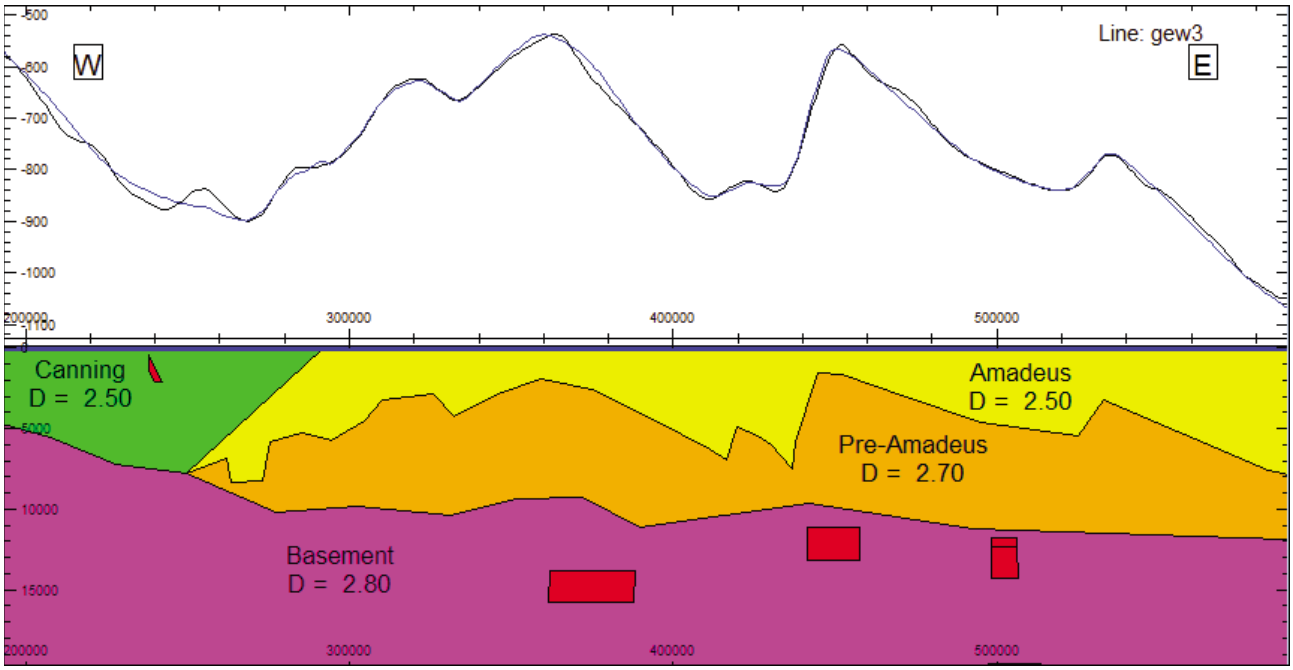

Figure 27. Southernmost east-west gravity model line Gew_3.

Figure 28 shows the eight north-south model cross-sections, which together generate a close match to the gravity variation observed on traverses along their central axes. There is generally smooth and modest variation between adjacent sections, consistent with the general east-west trend of the basin and its bounding structures. The only substantial difficulty in matching the gravity and magnetic expressions of the basin was over the northern basin margin on the easternmost section Gns_9, where the gravity-defined margin appears to be over 10 km to the north of the southernmost sharp, high-amplitude magnetic anomalies. This apparent discrepancy was resolved by introducing an over-thrust of shallow basement over the basin. Further effort may find an alternative solution, but this was not pursued, as it is a peripheral part of the model, outside the focus area of this study.

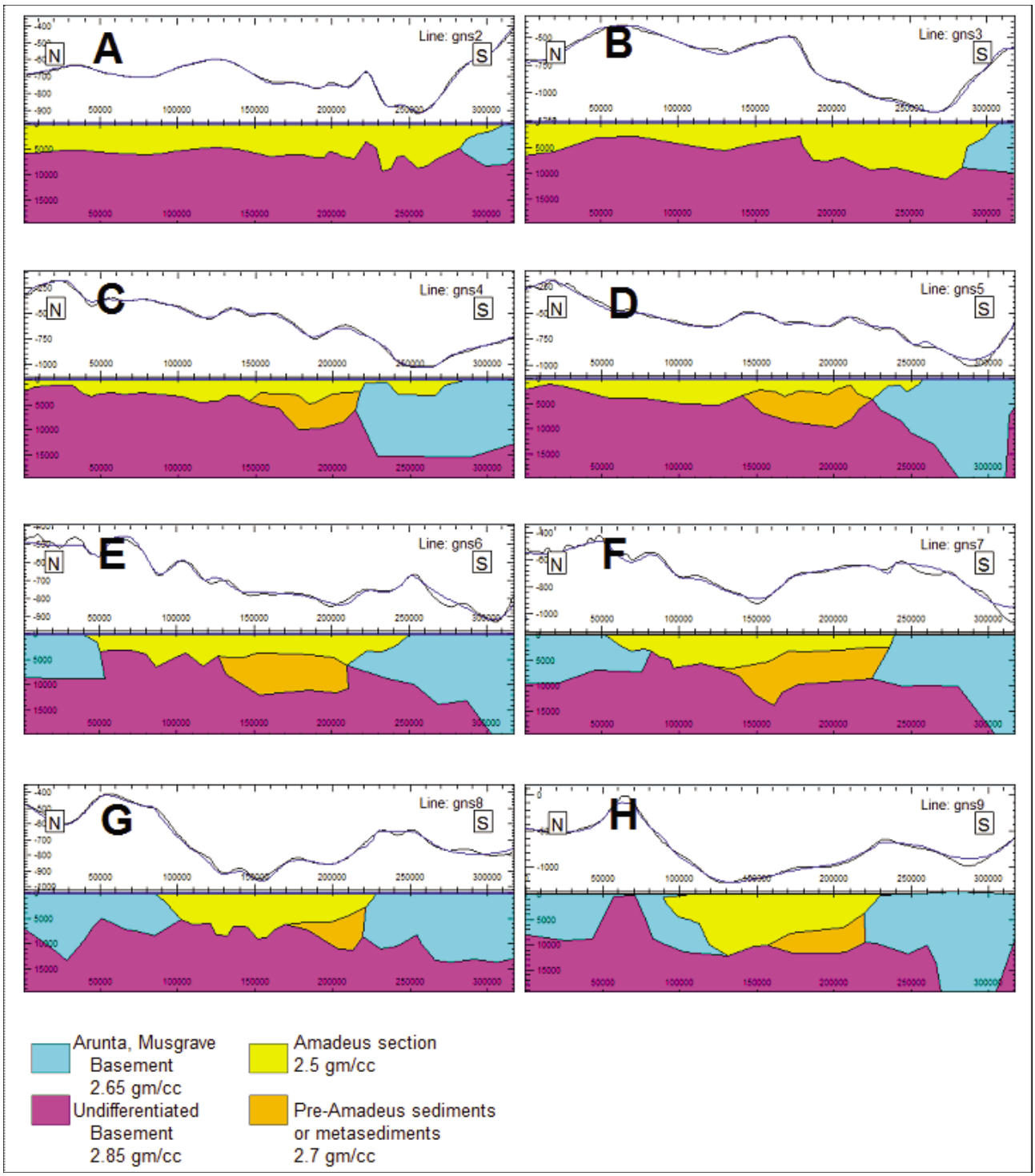

Figure 28. Final gravity model north-south sections (A to H is west to east). The observed Bouguer gravity is shown in black, and the model computed gravity in blue.

The intersection of the east-west and north-south model sections is shown in Figure 29. There is quite a close match at the traverse intersections, because the initial east-west model met its objective of supplying an approximate explanation of the gravity variation across this part of the basin. There was no attempt to resolve the small misfits at the intersections, as the east-west sections model was abandoned in favour of the subsequent, more definitive north-south sections model. The east-west variation in the basin structure, difficult to trace between the individual north-south sections, is shown in the block model in Figure 30, where the sedimentary rock units have been stripped away to reveal the basement structure. This figure shows the tentative modelling of a possible thin basement overthrust at the north-eastern end of the basin model.

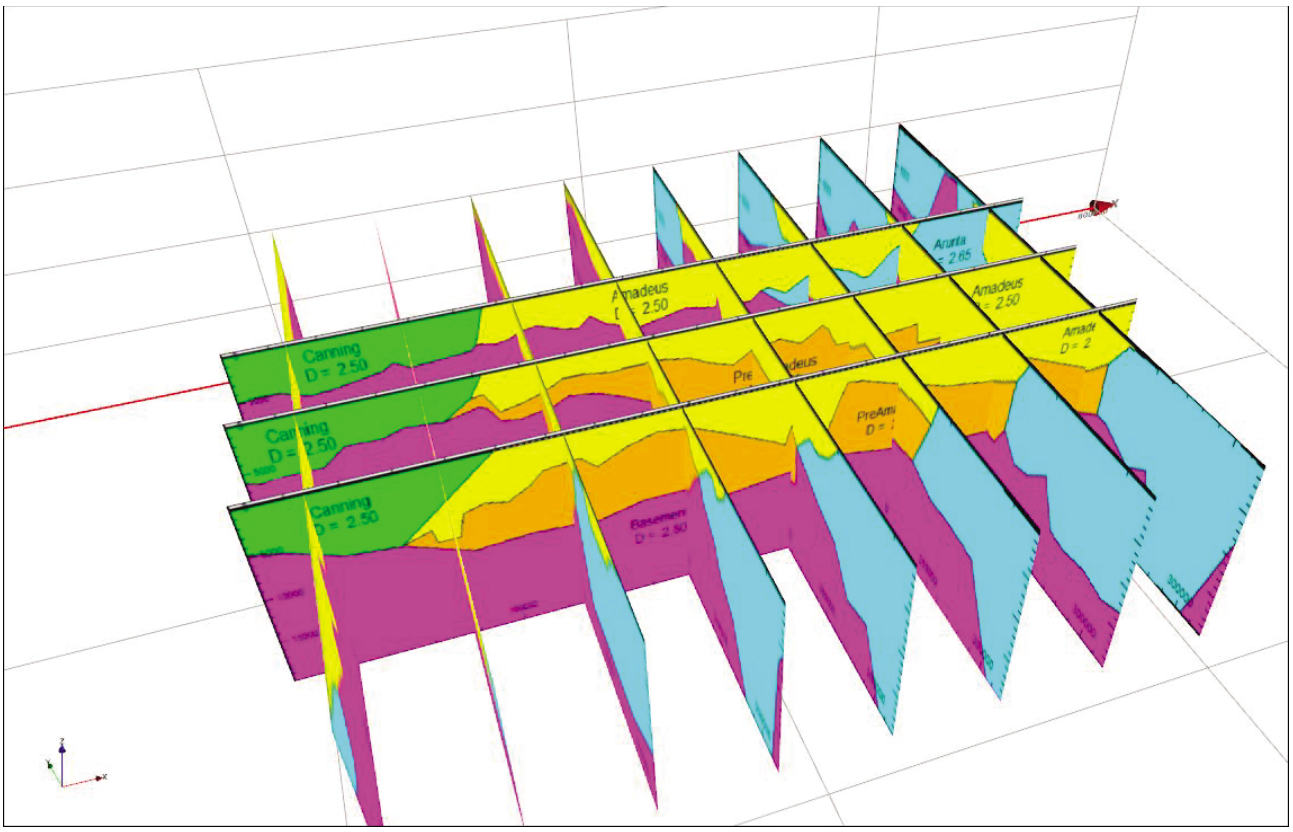

Figure 29. Intersection of the initial model east-west sections, and final model north-south sections (seen from the southwest).

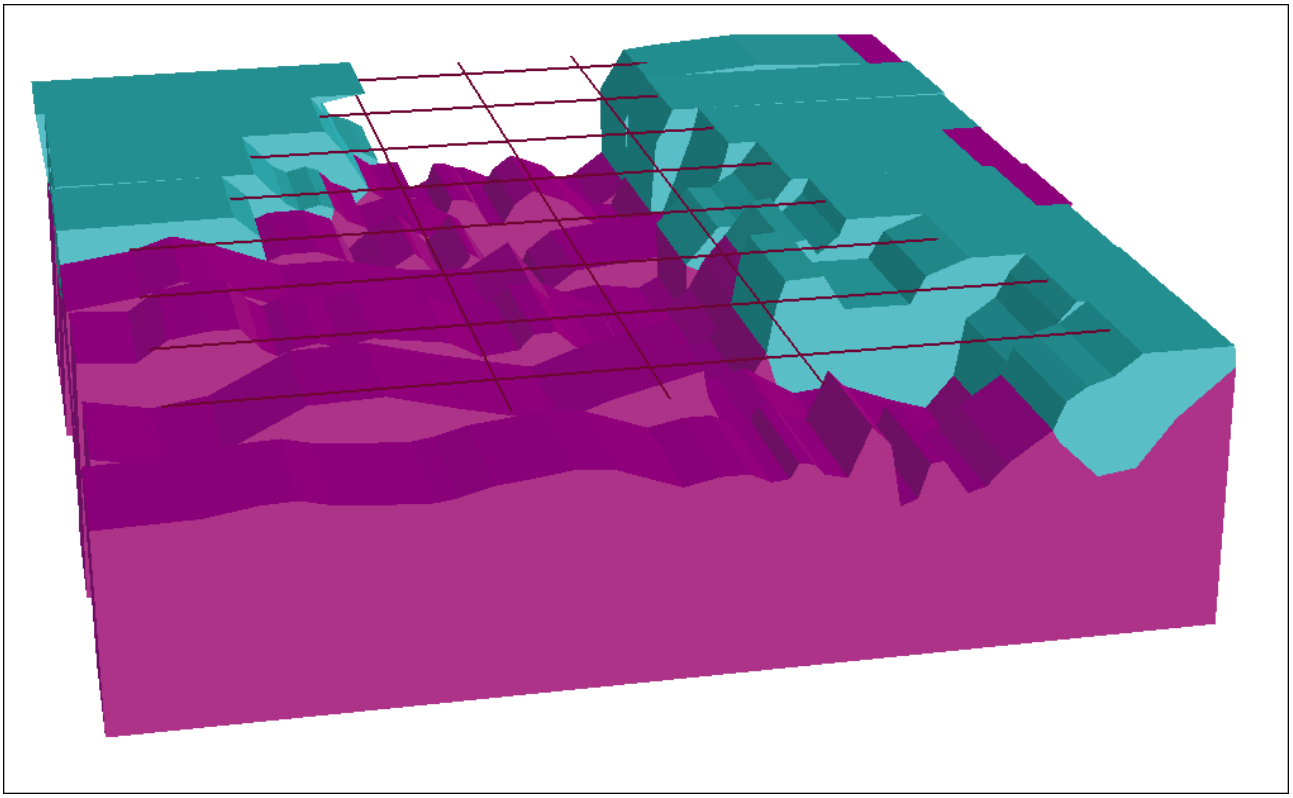

Figure 30. Block model of basement (purple – undifferentiated basement, blue – upper Musgrave and Arunta basement).

Figure 31 shows interpreted thickness of the Amadeus and Canning sections, generated by gridding the vertices on the base of the Amadeus and Canning section model units. The maximum thickness of Amadeus Basin section is at the far eastern end of the model, with depths in excess of 8 km at longitude 130° east, shallowing westwards to depths of about 4.5 kilometres at longitude 128° east. Further west, at the interpreted junction between the Canning and Amadeus basins, there is a broad, north-south basement ridge, shallowing to depths of less than 3 kilometres, before deepening westward into the Canning Basin. The smoothness of this interface is due in part to the coarse gridding across model transects at 50 km spacing. Modelling along the traverses themselves indicates sharp topography on this surface, which is probably at least in part defined by block faults, but it is difficult to trace those features between adjacent traverses.

The greater depths to crystalline basement are mapped in Figure 32. This result suggests that the central and southern parts of the basin have a significantly deeper crystalline basement than the northern part of the basin, but this deeper surface is less well constrained, and more speculative. Consistent with the magnetic source depths, which in part determined this surface, depths locally exceed 10 kilometres.

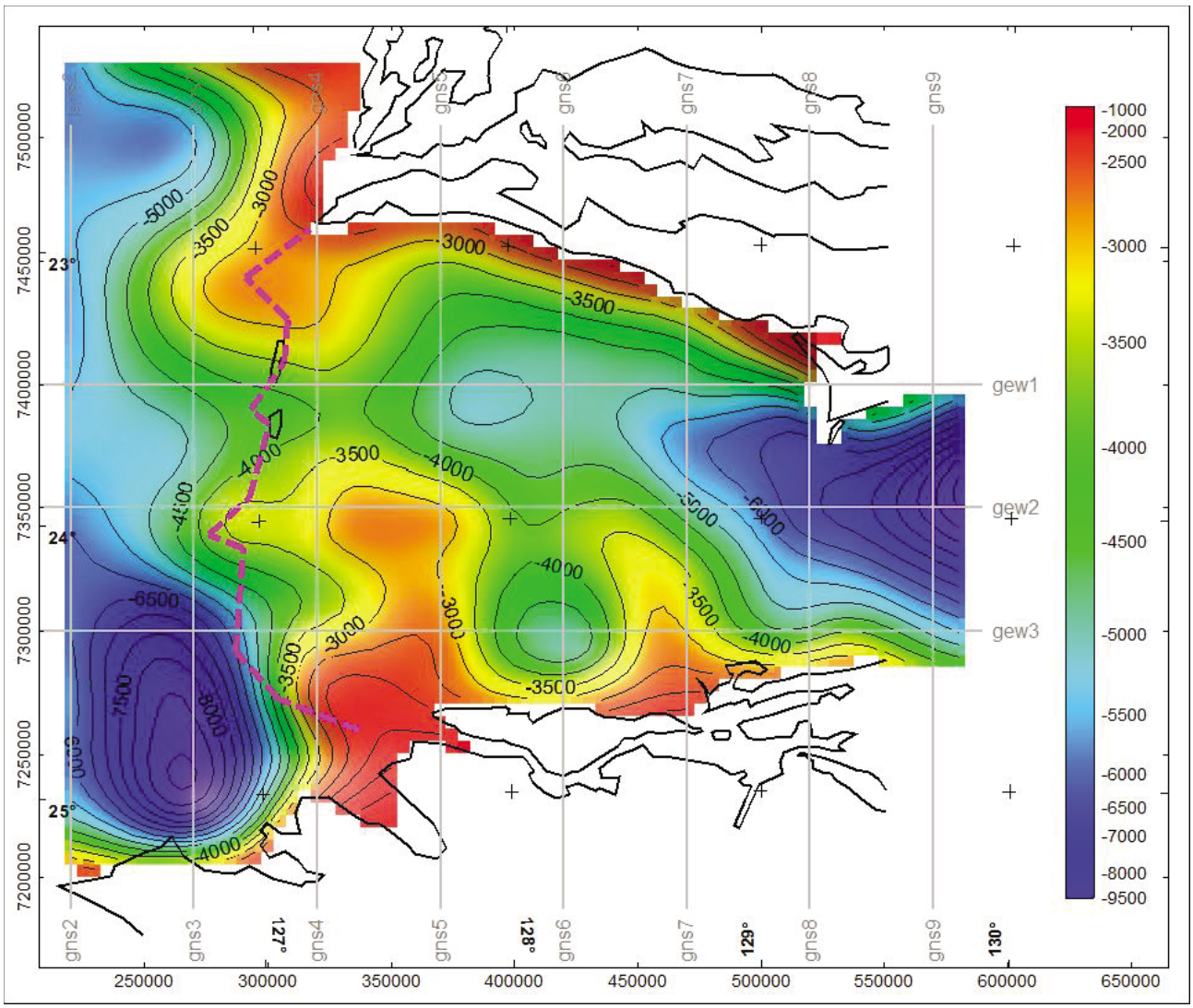

Figure 31. Modelled depth of Canning and Amadeus Basin section, generated by gridding the vertices defining the base of those model components. The dashed purple line shows the possible junction between the basins, as interpreted from the magnetic field data.

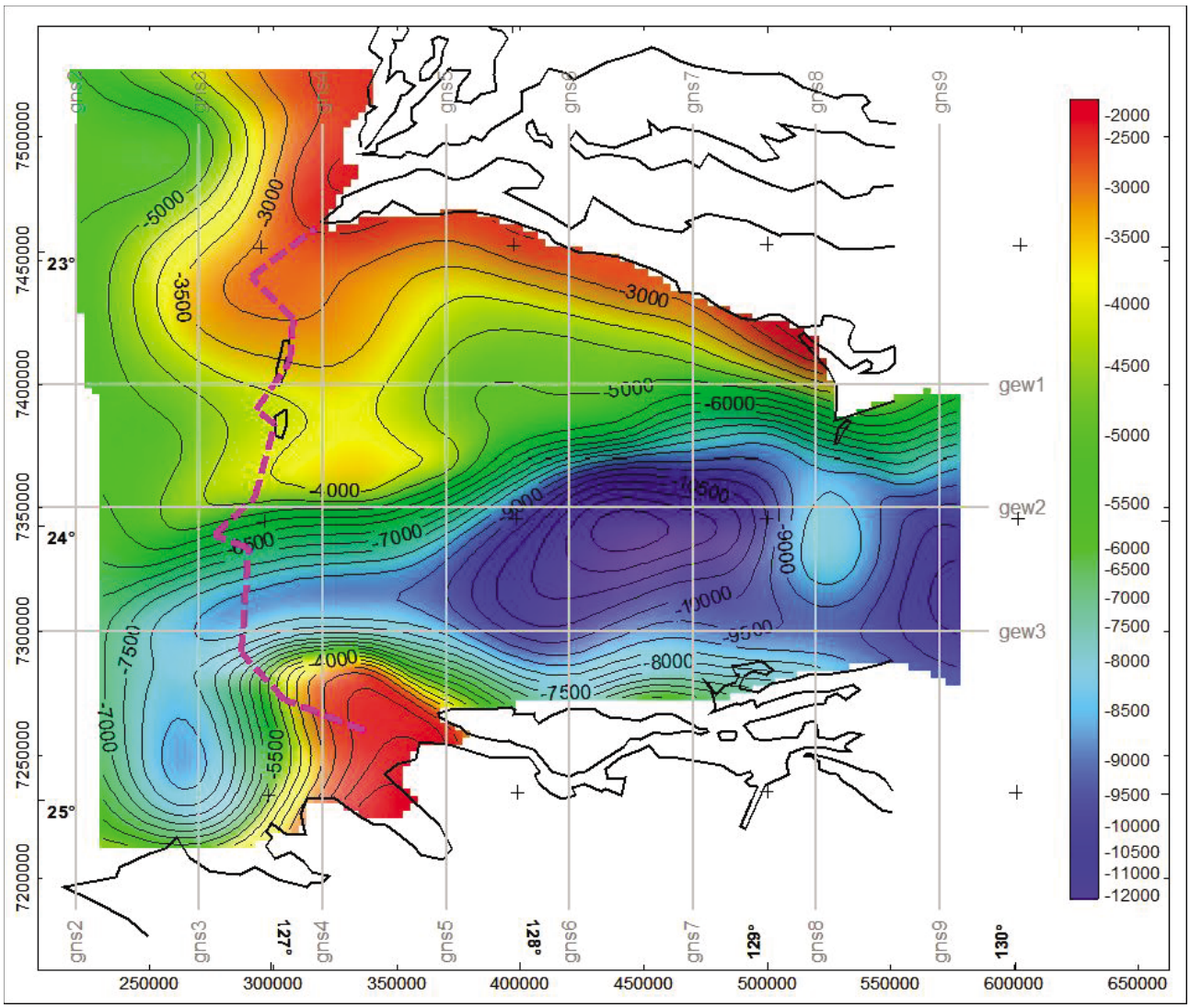

Figure 32. Modelled depth to basement, generated by gridding the vertices defining the top of modelled basement beneath the Amadeus and eastern Canning basins. The difference from Figure 31 is that this surface is beneath, rather than above, the modelled pre-Amadeus sediment/ meta-sediment.

6 Conclusions

A model for the western margin of the Amadeus Basin is proposed, primarily from interpretation of regional gravity and magnetic data. The final model generated from 50 km wide north-south strips with cross-sections as shown in Figures 28, 29 and 30, provides an approximate match to the observed gravity variation over the western section of the Amadeus Basin, but for reasons already discussed, this model is not unique, and there are many other models which could fit the data just as well, or better. Indeed, given the lack of hard constraints on the model, it is likely to have major failings as a representation of the true geology. It is also undoubtedly inaccurate to display such large volumes of complex geology as apparently homogeneous, but without independent constraints there is no justification to embellish the model with unjustified complexity.

The major suggestions of the modelling are that the Amadeus Basin section has a maximum thickness within the study area of about 8 km at the eastern end of the model, shallowing westward to approximately 4.5 km in the centre of the model, and to less than 3 km over a broad basement ridge. The top of crystalline basement is believed to be substantially deeper over some parts of the basin, beneath a thick section of pre-Amadeus Basin sedimentary or metasedimentary rocks, with depths in places in excess of 10 km. The topography of this surface is based in large part on guidance from spot depths derived from inversion of magnetic field anomalies.

The model has been built in a very modular fashion, allowing it to be deconstructed, to add additional detail as new constraints become available, or to test alternative hypotheses. In particular, if better constraints become available on the shallow structure of the basin, for instance from new drilling or seismic data, the single model layer representing a homogeneous basin section can be replaced with multiple stratigraphic layers, with the deeper part of the model then adjusted as necessary, to re-establish the match with the observed gravity data.

References

Aitken, AR, Dentith, MC, Evans, SF, Gallardo, LA, Joly, A, Thiel, S, Smithies, RH and Tyler, IM, 2013. Imaging crustal structure in the west Musgrave Province from magnetotelluric and potential field data: Geological Survey of Western Australia, report 114, 81 p.

Haines PW, Hand M & Sandiford M, 2001. Palaeozoic synorogenic sedimentation in central and northern Australia: a review of distribution and timing with implications for the evolution of intracontinental orogens. Australian Journal of Earth Sciences 48, 911-928.

Joly, A, Dentith, MC, Porwal, A, Spaggiari, CV, Tyler, IM and McQuaig, TC, 2013. An integrated geological and geophysical study of the west Arunta Orogen and its mineral prospectivity: Geological Survey of Western Australia, Report 113, 89p.

Korsch, RJ & Lindsay JF, 1989. Relationship between deformation and basin evolution in the intracratonic Amadeus Basin, central Australia. Tectonophysics 158, 5-22.

Neumann, N.L. (d.) 2013. Yilgarn Craton-Officer Basin-Musgrave Province Seismic and MT Workshop. Record 2013/28. Geoscience Australia: Canberra.

Smithies RH, Kirkland CL, Korhohen FJ, Aitken ARA, Howard HM, Maier WD, Wingate MTD, de Gromard QR, and Gessner K, 2013. The Mesoproterozoic thermal evolution of the Musgrave province in central Australia – Plume vs. The geological record, Gondwana Research.

Walter, MR, Veevers, JJ, Calver, CR and Grey, K 1995. Neoproterozoic stratigraphy of the Centralian Superbasin, Australia: Precambrian Research, v. 73, p. 173–195.

Wells, AT, Forman, DJ, Ranford, LC and Cook, PJ 1970. Geology of the Amadeus Basin, central Australia: Australia BMR, Bulletin 100, 222p.

CONTACT US

t 1300 363 400
+61 3 9545 2176
e enquiries@csiro.au
w www.csiro.au

YOUR CSIRO

Australia is founding its future on science and innovation. Its national science agency, CSIRO, is a powerhouse of ideas, technologies and skills for building prosperity, growth, health and sustainability. It serves governments, industries, business and communities across the nation.

FOR FURTHER INFORMATION

CSIRO-MRF
Dr Clive Foss
t +61 2 9490 8713
e clive.foss@csiro.au

CSIRO-MRF
Dr James Austin
t +61 2 9490 8876
e james.austin@csiro.au

CSIRO MRF
Dr Susanne Schmid
t +61 8 6436 8801
e susanne.schmid@csiro.au

This Report presents a structural model of the poorly exposed and undrilled western Amadeus Basin derived primarily from the interpretation of regional gravity and magnetic data. It is concluded that within the modelled area the Amadeus Basin section has a maximum thickness of about 8 km at the eastern end, shallowing westward to approximately 4.5 km in the centre, to less than 3 km over a broad north–south trending basement ridge at the western end. The top of crystalline basement is believed to be substantially deeper over some parts of the basin, beneath a thick section of magnetically transparent pre-Amadeus Basin sedimentary or metasedimentary rocks, with depths in places exceeding 10 km. The topography of this surface is based in large part on guidance from spot depths derived from inversion of magnetic field anomalies.

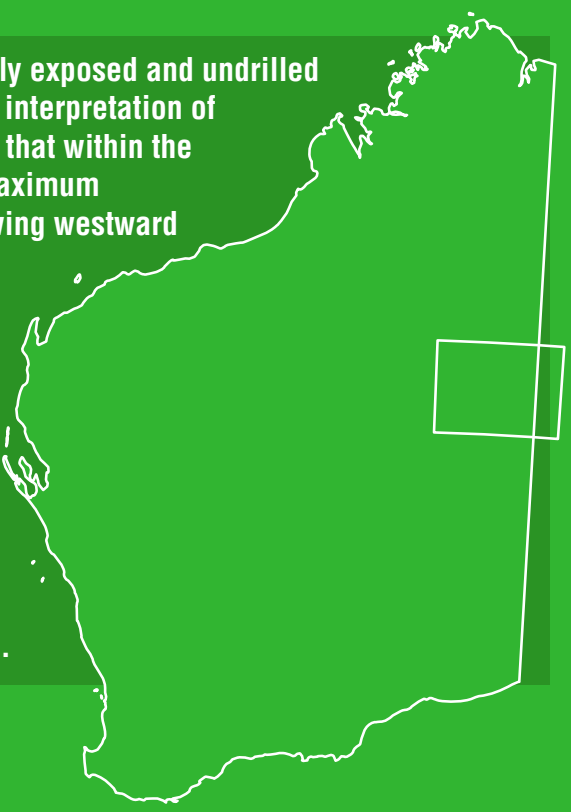

Further details of geological products and maps produced by the Geological Survey of Western Australia are available from:

Information Centre
Department of Mines and Petroleum
100 Plain Street
EAST PERTH WA 6004
Phone: (08) 9222 3459 Fax: (08) 9222 3444

www.dmp.wa.gov.au/GSWApublications

FOSS et al.

COBRA — AMADEUS BASIN PROJECT: GRAVITY AND MAGNETIC STUDY OF THE WESTERN AMADEUS BASIN, WESTERN AUSTRALIA

REPORT 154